Electronic Supplementary Material (ESI) for Journal of Materials Chemistry A.

Supporting Information

Enhanced Proton Conduction by Post-Synthetic Covalent Modification in a Porous Covalent Framework

Partha Samanta,[‡a] **Aamod V. Desai,**[‡ a] **Bihag Anothumakkool,**[b] **Mandar M. Shirolkar,**[c] **Avishek Karmakar,**[a] **Sreekumar Kurungot,**[b] **and Sujit K. Ghosh***[a]

[a]Department of Chemistry, Indian Institute of Science Education and Research, Pune, E-mail: sghosh@iiserpune.ac.in

[b] Physical and Materials Chemistry Division, National Chemical Laboratory (NCL),Pune 411 008, India.

[c] Hefei National Laboratory for Physical Science at the Macroscale, University of Technology of China.

Department of Physics, Tamkang University, Tamsui, 251, Taiwan (Present address)

Experimental Section:

Electrochemical Impedance Analysis: Impedance analysis of the samples was carried out in Bio-Logic VMP-3. Measurements were done in a two-electrode assembly with stainless steel discs as electrode and pelletized samples (13mm diameter and prepared by 10ton pressure) were kept in between them in the form of solid pellets by applying a spring load of 0.5 N/m^2. The whole cell assembly was kept in Espec environmental test chamber to control the temperature and relative humidity. Applied frequency range for the measurement was from10^{-6} to 0.1 Hz against the open circuit potential with sinus amplitude of 10 mV. All the EIS data were fitted using an EC-Lab Software V10.19 using equivalent circuit as shown below

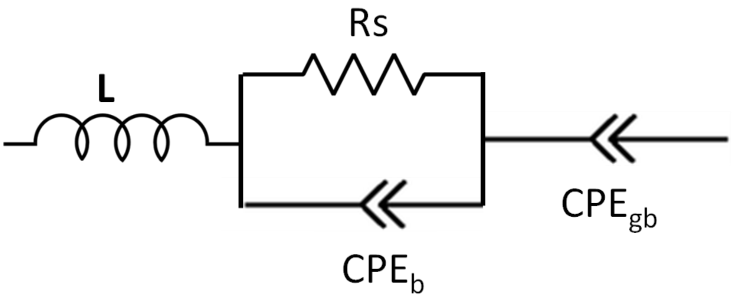

Where L is inductance (H), R_s is the bulk resistance (Ω) of the pellet, CPE_b and CPE_{gb} are the non-ideal capacitance for bulk and non-ideal capacitance for grain boundary (F.S^{a-1}).Further, R_s is used to find the conductivity of the sample by considering the area and thickness of the sample.

FE-SEM analysis: <1 mg of each sample was dispersed in dry $CHCl_3$ via 10 minutes sonication and then was loaded on silicon wafer which was then used for FE-SEM imaging after drying overnight. For solid-state analysis <1 mg sample was adhered on double sided carbon tape and hence used for FE-SEM imaging. FESEM was done by using FEI Quanta 3D dual beam ESEM at 30KV.

Structural simulation Study: Materials Studio software suite 8.0 (Accelrys) has been used to perform the structural simulations. Initially, the molecular structure of the building units was fully relaxed using Discover module and the structural simulation on the relaxed structure was performed using Condensed – Phase – Optimized Molecular Potentials for Atomistic Simulation Studies (COMPASS) force fields. A Connollly surface was created for the model using Atom, Volumes and Surface tool in Materials Studio with a fine grid resolution (0.25 Å) and a Connolly radius set to 1.82 Å. The sorption isotherms were modeled using the Sorption module available within Materials Studio. N_2 sorption isotherms were calculated at 77 K. The Universal forcefield was used at a fine-quality calculation level for isotherm calculations.

Electrical Conductivity Measurement: Electrical conductivity was measured with the pelletized sample by conventional two probe method.

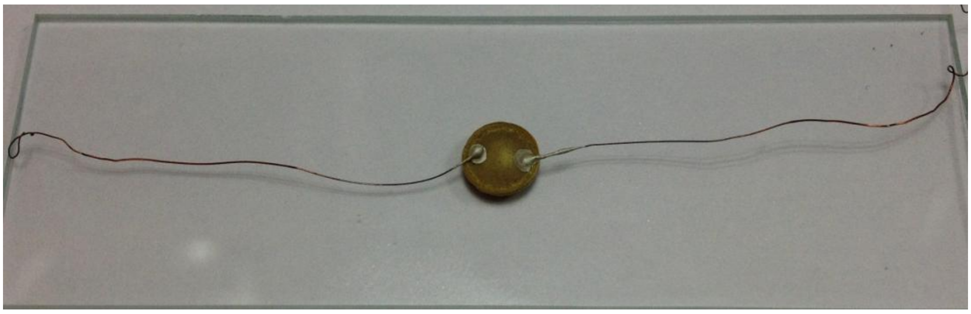

Pelletized Sample

Synthesis of 2,4,6-tris(4-fluorophenyl)-1,3,5-triazine (TFPT): A solution of 4-fluorobenzonitrile (3.5 g, 28.8 mmol) in dry $CHCl_3$ (15 mL) was added to a stirred solution of trifluoromethanesulfonic acid (11 mL, 124.6 mmol) in dry $CHCl_3$ (30 mL) at 0 ^oC. The stirring was continued for 2 hours at 0 ^oC and further at room temperature for 48 hours. The mixture was then poured into water containing a small amount of sodium bicarbonate. The chloroform layer containing TFPT was rinsed with water several times and dried *in vacuo*. Solid white coloured compound was isolated which was recrystallised from chloroform for further use. Yield: 2.9 g, 83.9%.

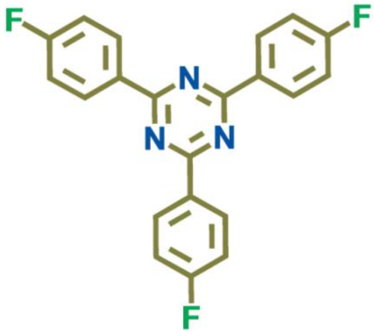

ESI m/z 364.1062 (Calculated Mass: $(M+H)^+$ 364.1061).

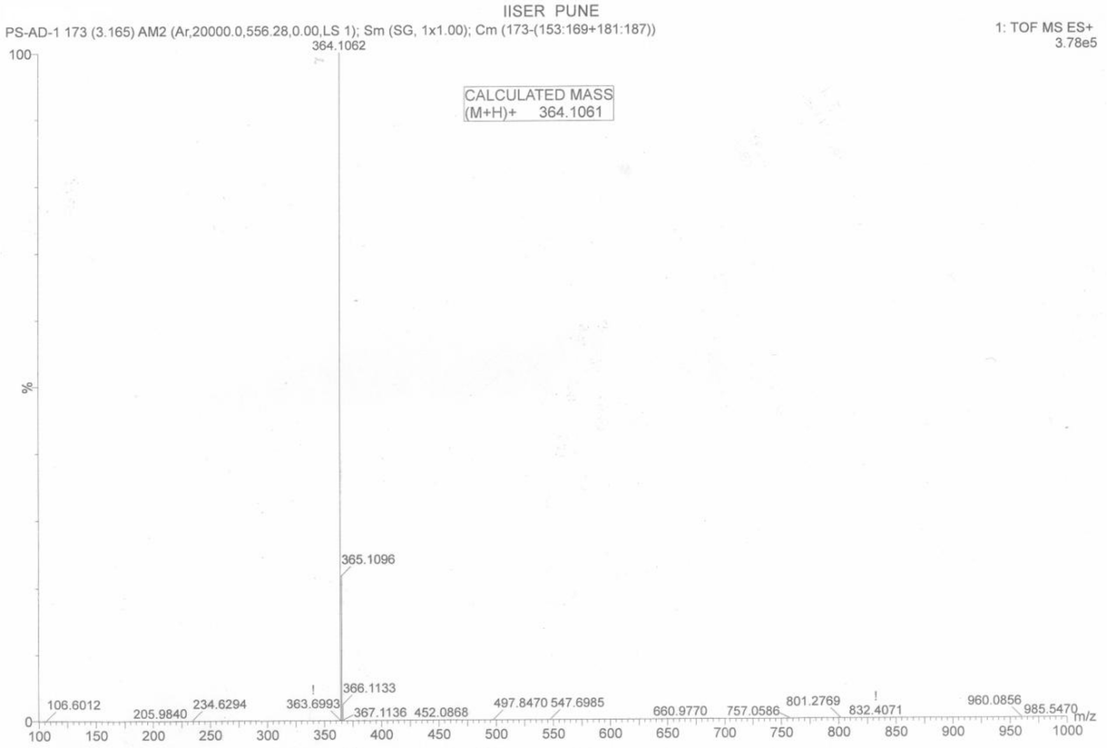

Figure S1: HRMS spectrum of 2,4,6-tris(4-fluorophenyl)-1,3,5-triazine (TFPT).

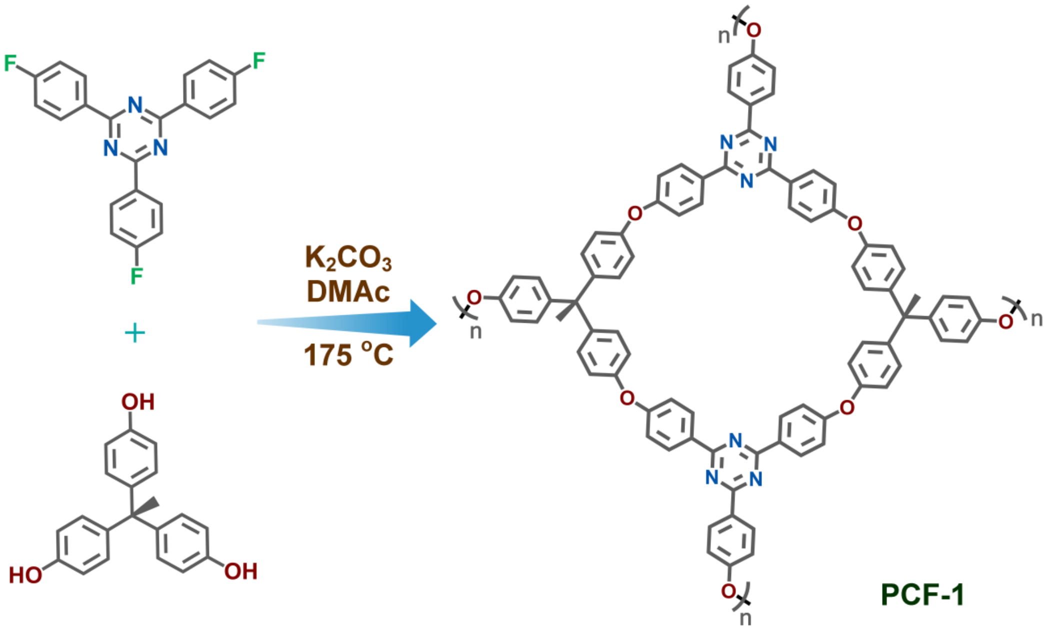

Scheme S1: Synthesis of PCF-1.

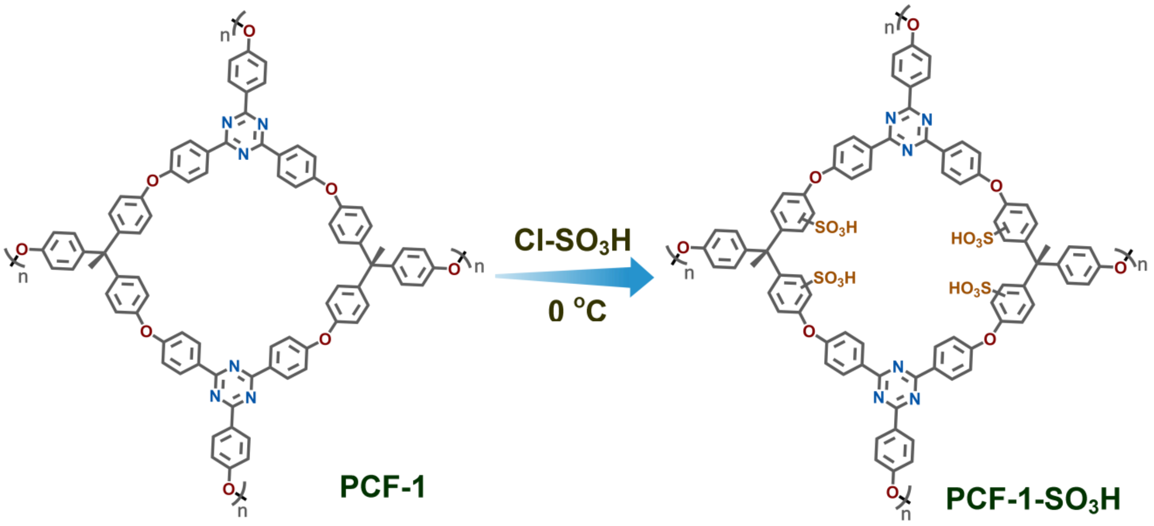

Scheme S2: Synthesis of PCF-1-SO$_3$H.

Synthesis of monomer (Mono-1): A round bottom flask was charged with TFPT (0.5 g, 1.37 mmol), 4-methoxyphenol (0.51 g, 4.11 mmol) and potassium carbonate (1.13 g, 8.22 mmol). To this solid mixture, DMAc (25 mL) was added under nitrogen atmosphere and the reaction was gradually heated to reflux. The stirring was continued for 24 hours at this condition. Upon cooling the mixture was concentrated under vacuum and the compound was extracted with DCM and washed with water several times. The organic layer was then reduced *in vacuo* to yield off-white powder of Mono-1. The compound was recrystallized from DCM for further use. Yield: 2.9 g, 83.9%.

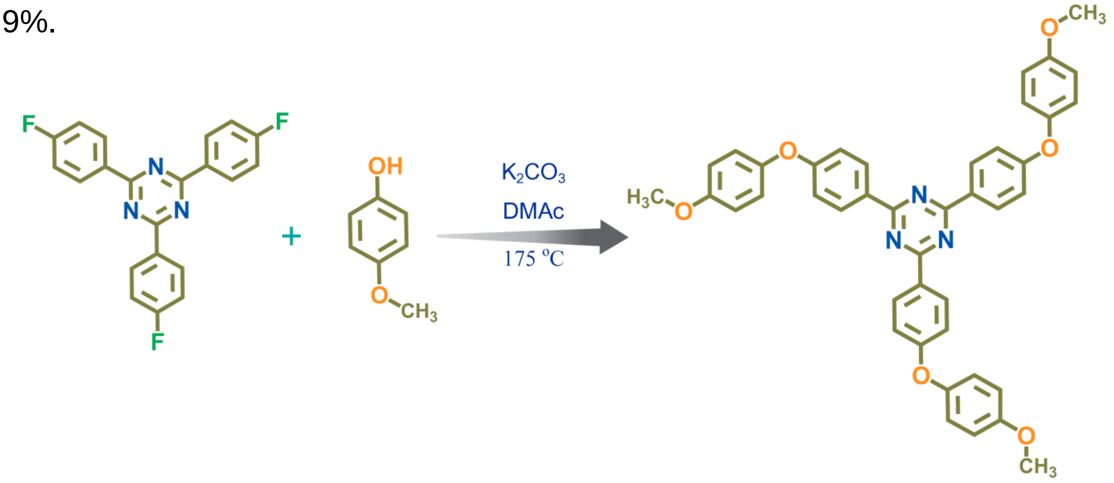

Scheme S3: Synthesis of monomer (Mono-1).

CCDC 1435226 (Mono1) contains the crystallographic data for this paper. These data can be obtained free of charge from The Cambridge Crystallographic Data Centre via www.ccdc.cam.ac.uk/data_request/cif.

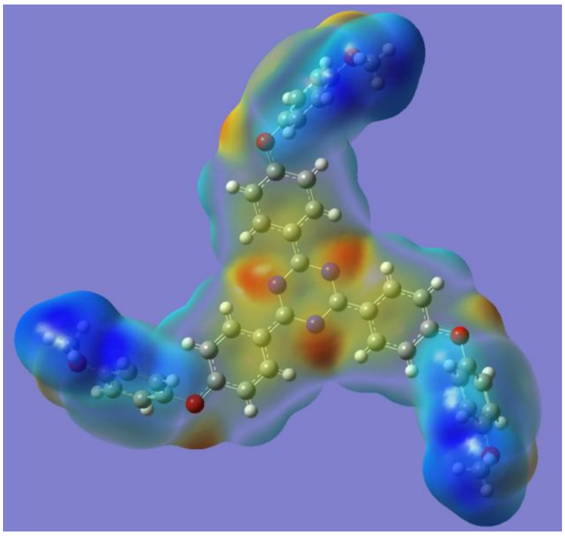

Figure S2: Electron density in monomer (Mono-1) where blue region denotes electron rich sites and red region indicates electron deficient sites.

Synthesis of sulfonated monomer (Mono-1): In a round bottom Mono-1 (250 mg, 0.37mmol) was taken and dissolved in 25 ml of DCM. Reaction mixture was cooled to 0 °C and kept at this condition for 15 minutes. A DCM solution of $Cl-SO_3H$ (0.22 ml, 3.33mmol) was added slowly to the Mono-1 solution. On completion of the reaction after 18 hours hexane was poured to the reaction mixture and kept for few hours. Then hexane was removed and toluene was poured to the reaction mixture and allowed to heat at 120 °C for overnight. Thus obtained solid mass was filtered and characterised with HRMS. ESI m/z 916.1140 (Calculated Mass: $(M+H)^+$ 916.1152).

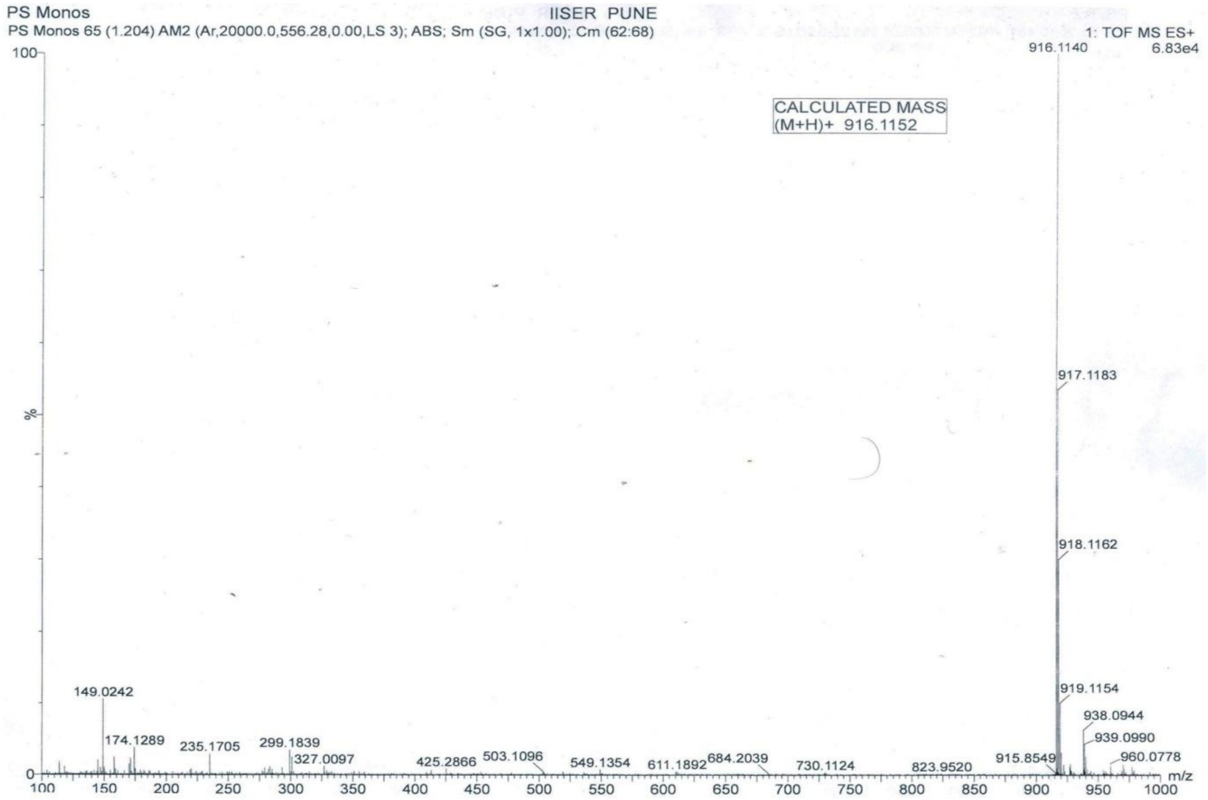

Figure S3: HRMS spectrum of sulfonated Mono-1.

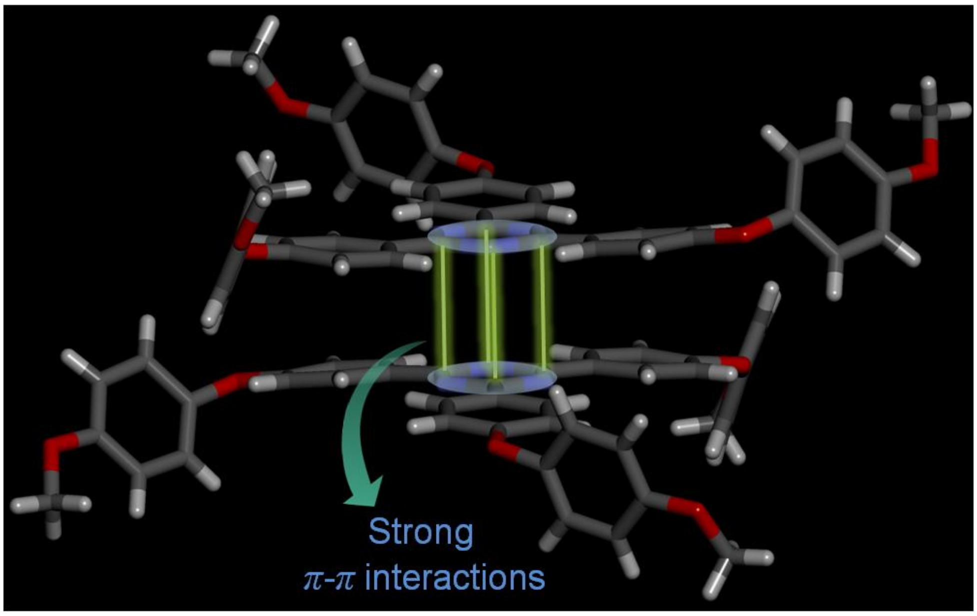

Figure S4: Stack view of Mono-1.

Extent of sulfonation in PCF-1:

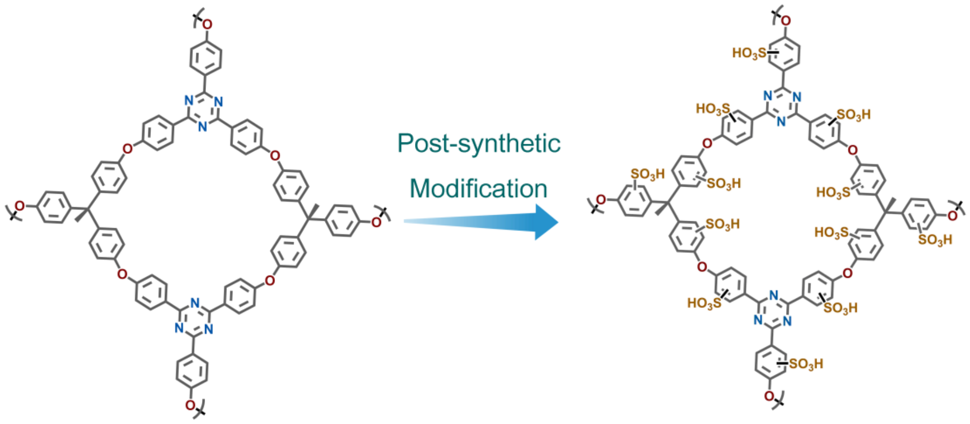

Observed:

% C	% H	% N	% S
76.67	3.317	7.26	0.0

% C	% H	% N	% S
54.49	3.403	5.183	6.941

Scheme S4: Speculation of extent of sulfonation in PCF-1 from elemental analysis.

In the repeating unit of PCF-1 total number of benzene rings are twelve. The C/N ratio obtained from the experimental values is 10.56. Upon sulphonation the C/N ratio is obtained as 10.51, which indicates that the framework is intact and the extent of sulphonation can be directly linked to the sulphur content. Here we have speculated the extent of sulfonation in PCF-1 by using the % of S obtained from elemental analysis (average % of S in three batches of PCF-1-SO_3H taken into account).

If, all twelve benzene rings got sulfonated, then expected % of S ≡ 15.61 % of S

But observed average % of S in PCF-1-SO_3H = 6.941 % of S

So, the extent of sulfonation in PCF-1-SO_3H ≡ (6.941/15.61) x 100

≡ 44.47% sulfonation occurred (~5.2 rings)

This value can be correlated to the observation for sulphonated monomer (Mono-1); wherein despite having 6 benzene rings, the sulphonation occurs at only 3 rings, most likely at the electron rich rings which are away from the triazine core. Also the size of the pore has to be taken into consideration for PCF-1-SO_3H which prevent complete sulphonation.

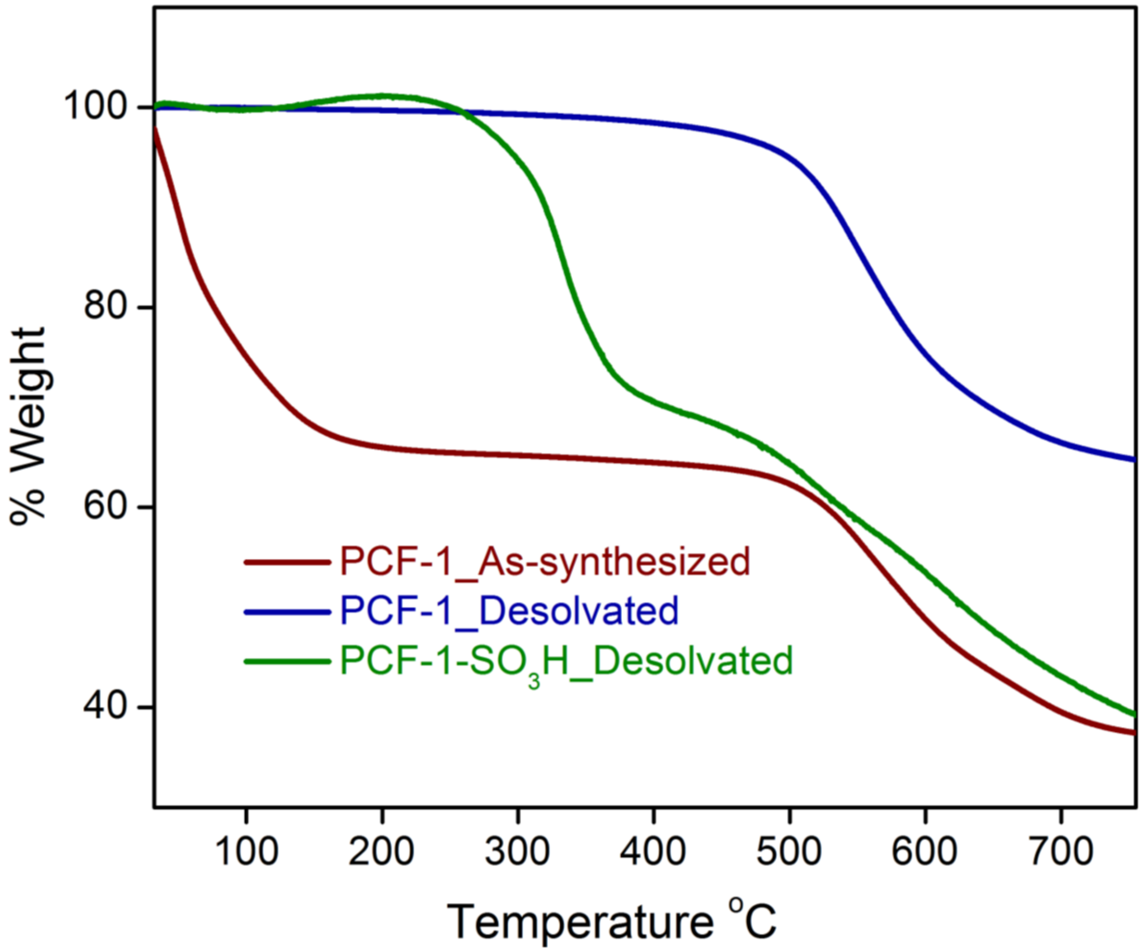

Figure S5: Thermogravimetric analysis of PCF-1 assynthesized (wine red), desolvated (blue) and desolvated PCF-1-SO_3H (green).

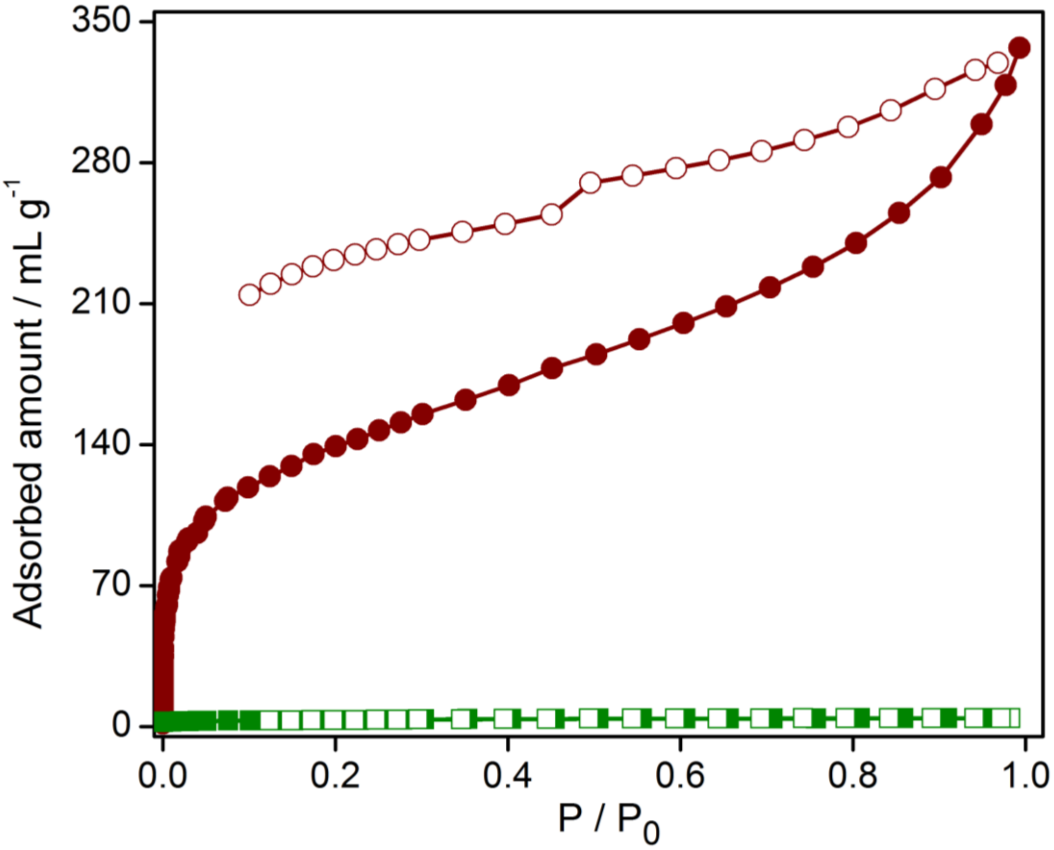

Figure S6: N_2 adsorption isotherm of PCF-1 (wine) and PCF-1-SO_3H (green) at 77 K.

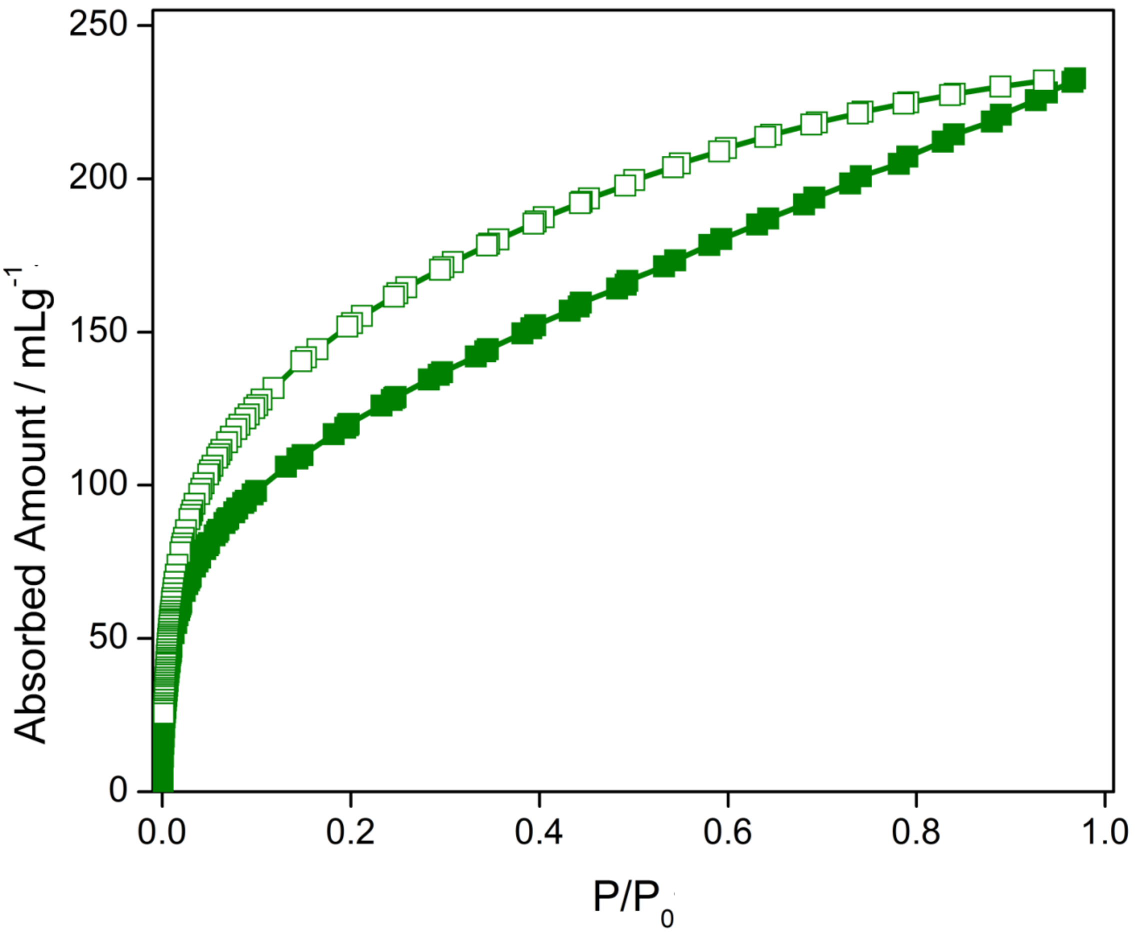

Figure S7: CO_2 adsorption isotherm of PCF-1 (green) at 195 K.

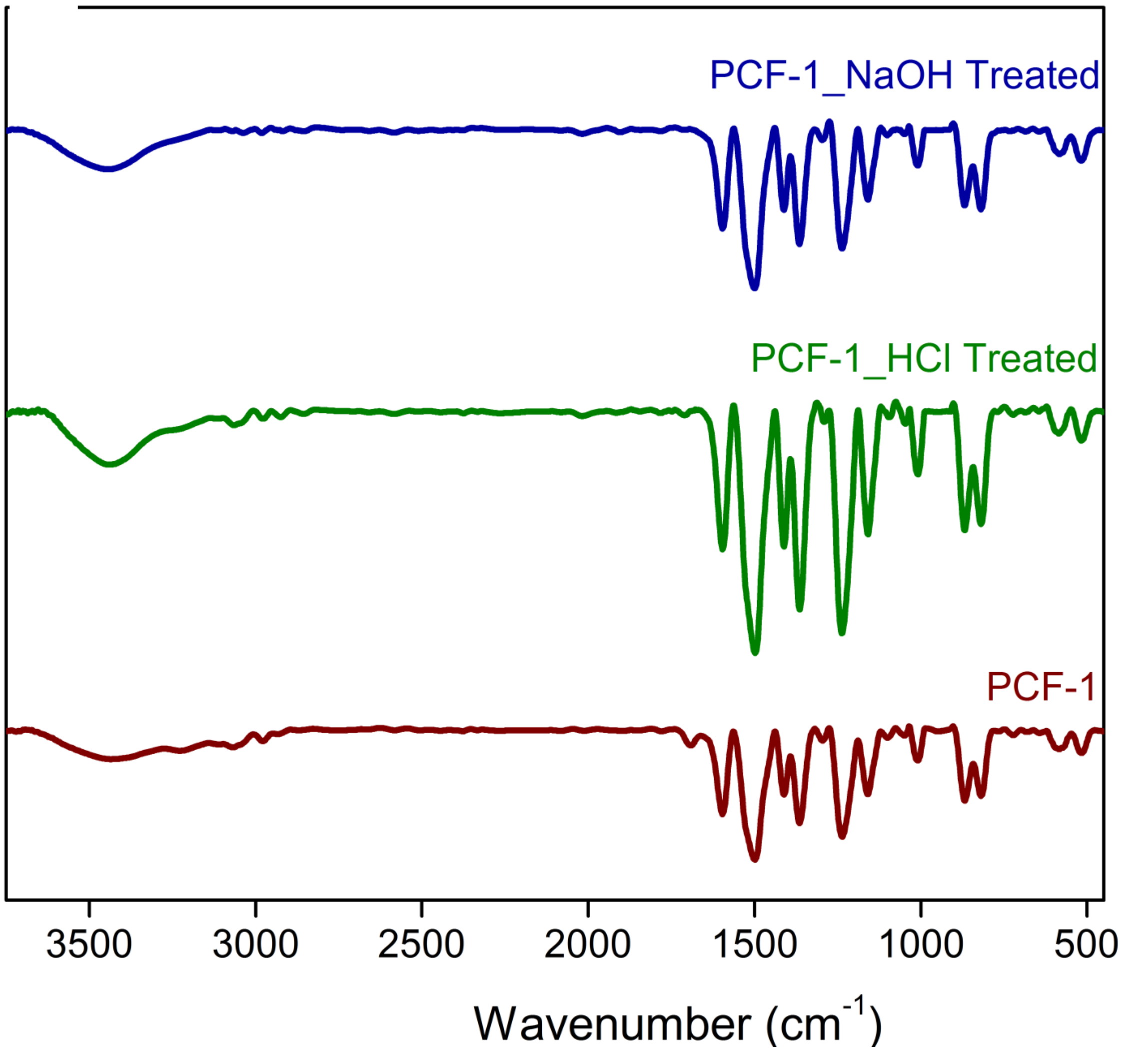

Figure S8: FT-IR spectra of PCF-1 (wine), PCF-1 acid treated (green) and PCF-1 base treated (blue).

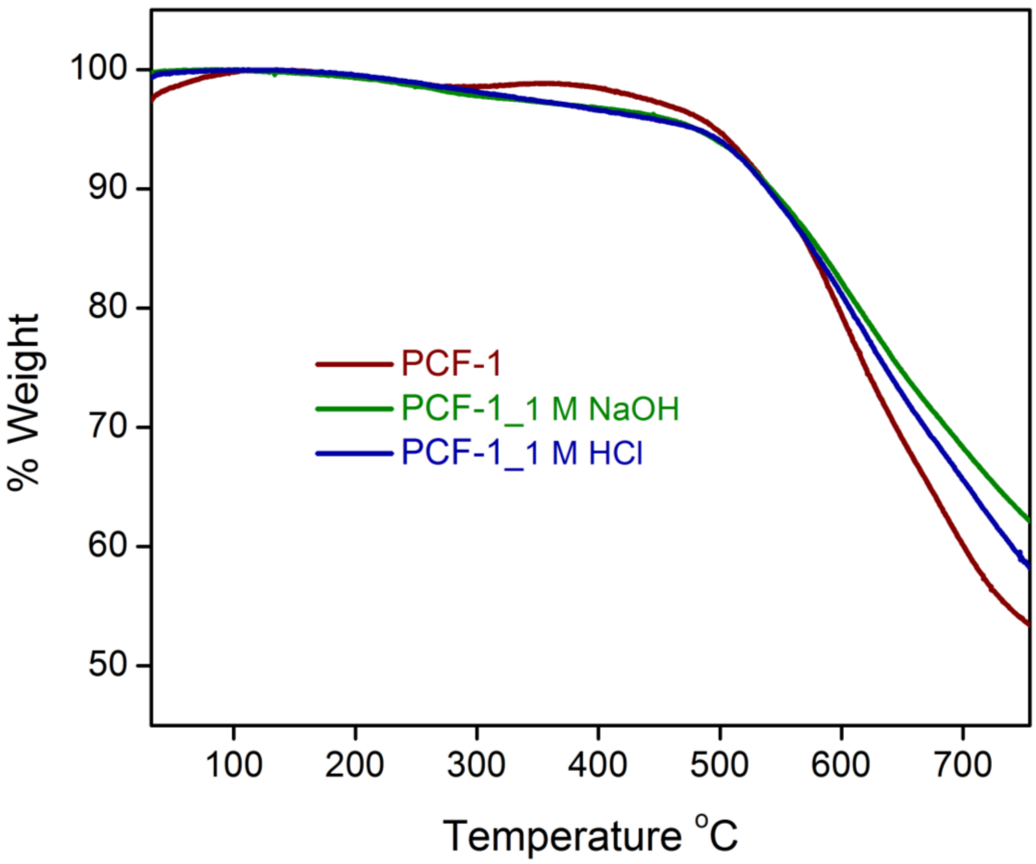

Figure S9: Thermogravimetric analysis (TGA) of PCF-1 (wine), PCF-1 acid treated (blue) and PCF-1 base treated (green).

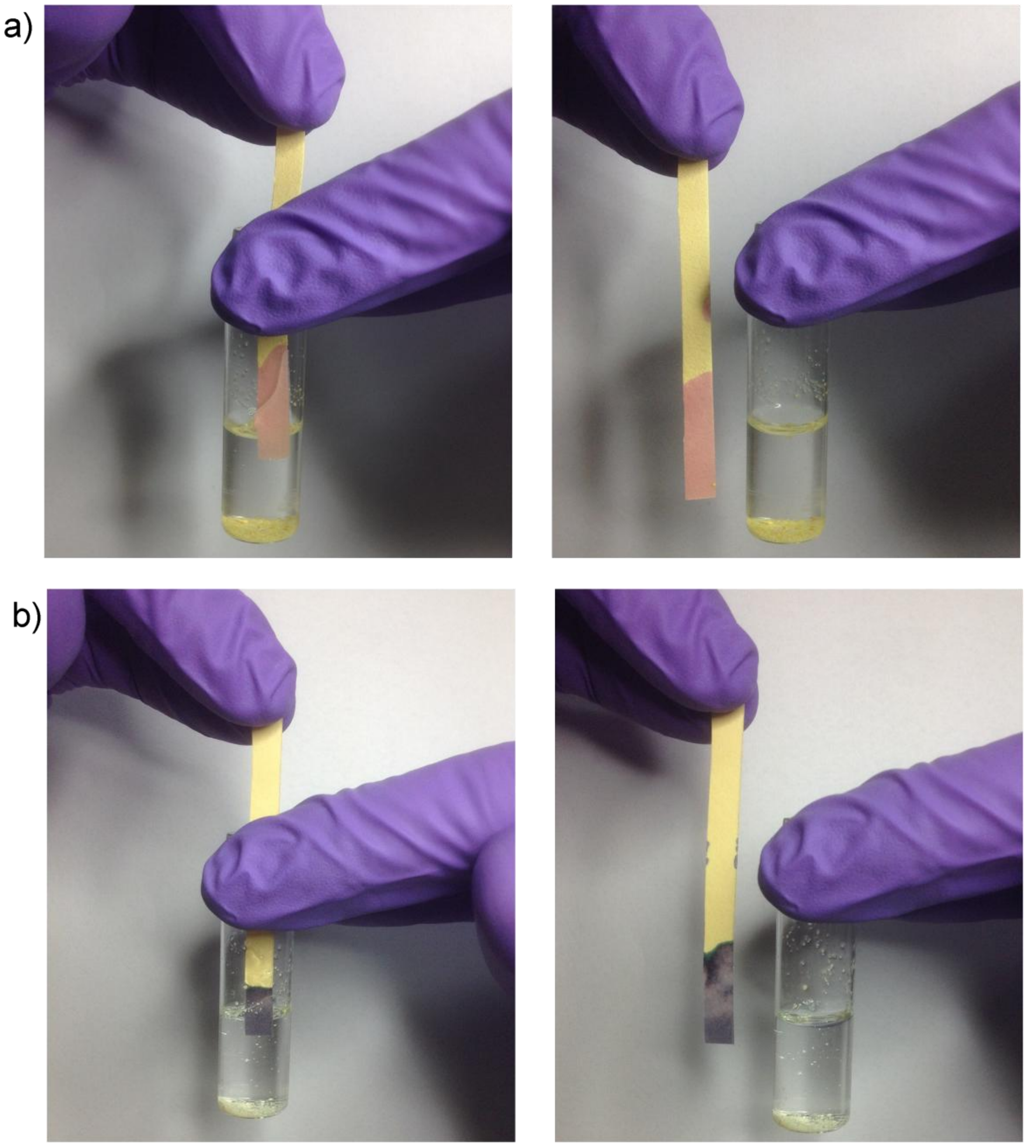

Figure S10: Photographs of a) acid dipped PCF-1 (1 M HCl) and b) base dipped PCF-1 (1 M NaOH).

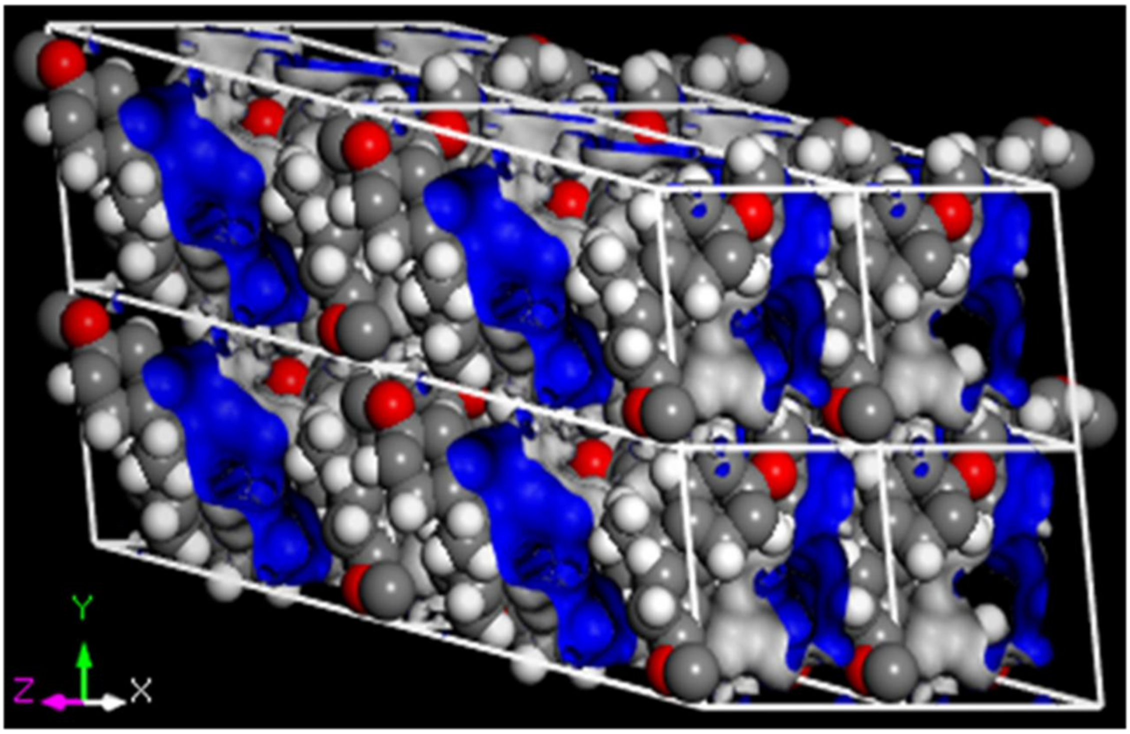

Figure S11: 3D array of (2×2×2) amorphous cells with periodic boundary conditions. A Connolly surface was shown in blue/gray. Connolly surface occupied Volume: 1521.29 Å³, Free Volume: 619.40 Å³ and Surface Area: 749.64 Å².

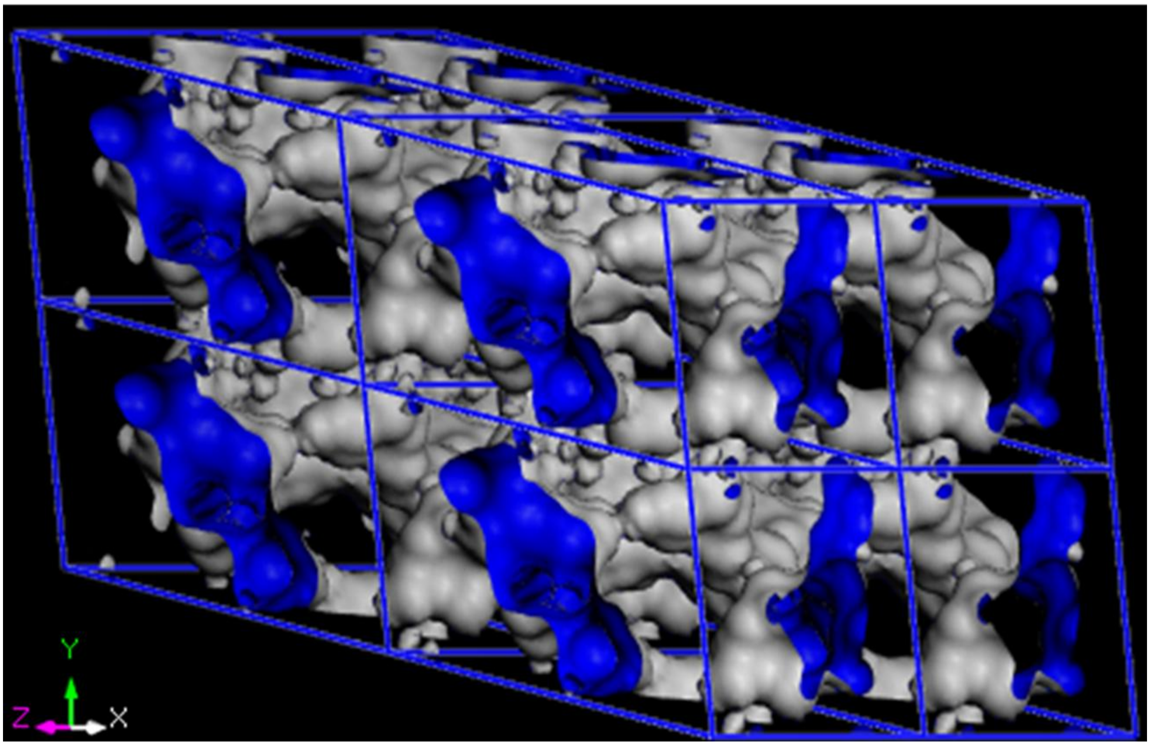

Figure S12: The occupied and unoccupied volume is shown in gray and blue respectively in simulated structure of PCF-1.

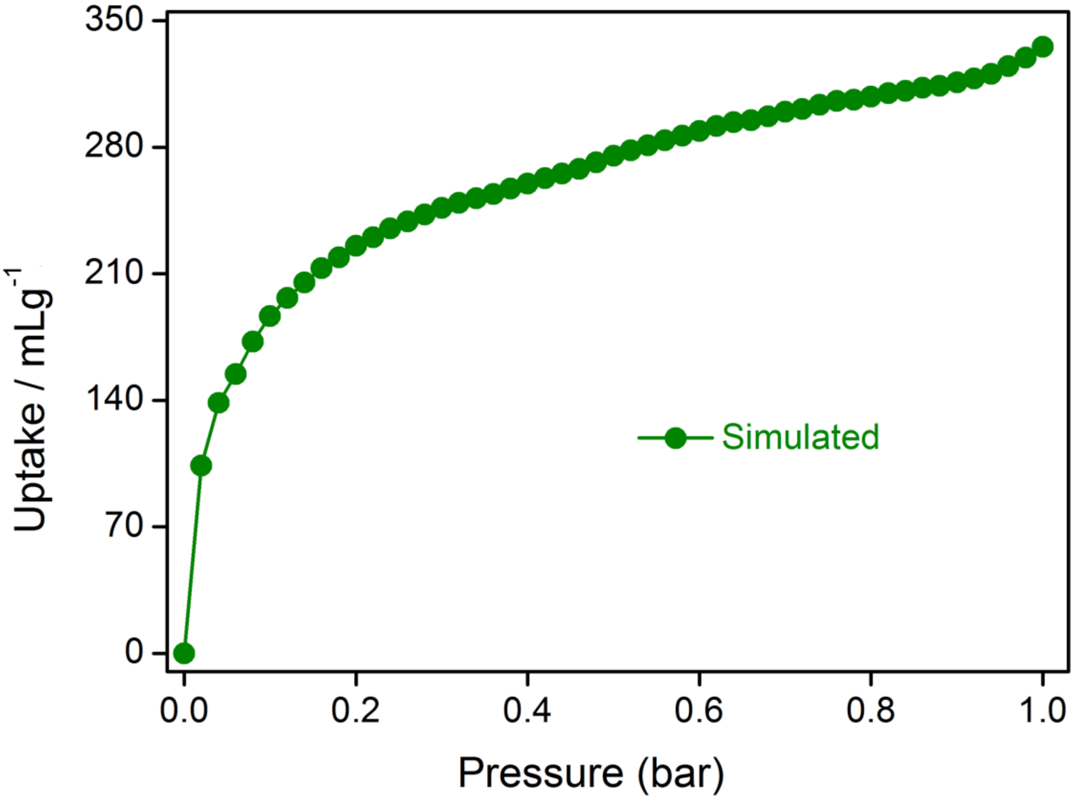

Figure S13: Simulated N_2 adsorption profile of PCF-1 at 77 K.

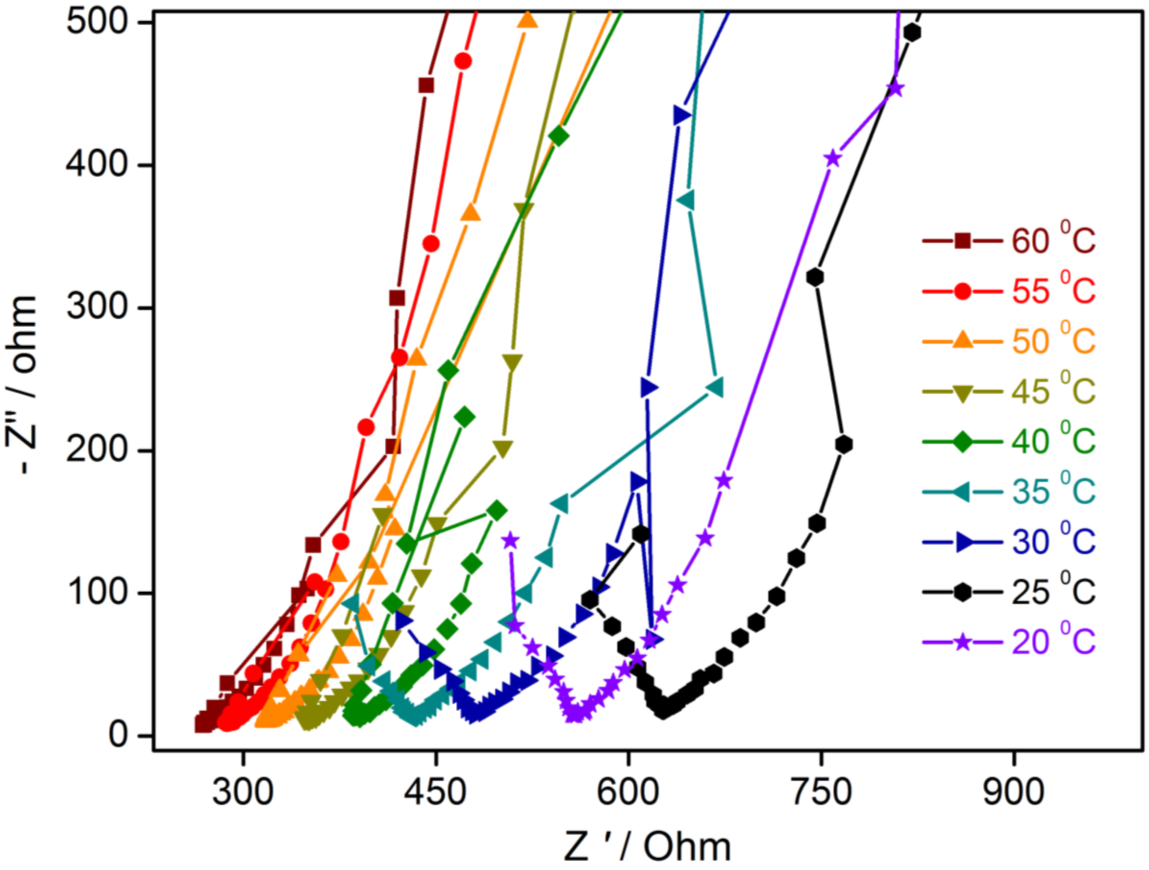

Figure S14: Temperature dependent impedance spectra of PCF-1 at 95% RH.

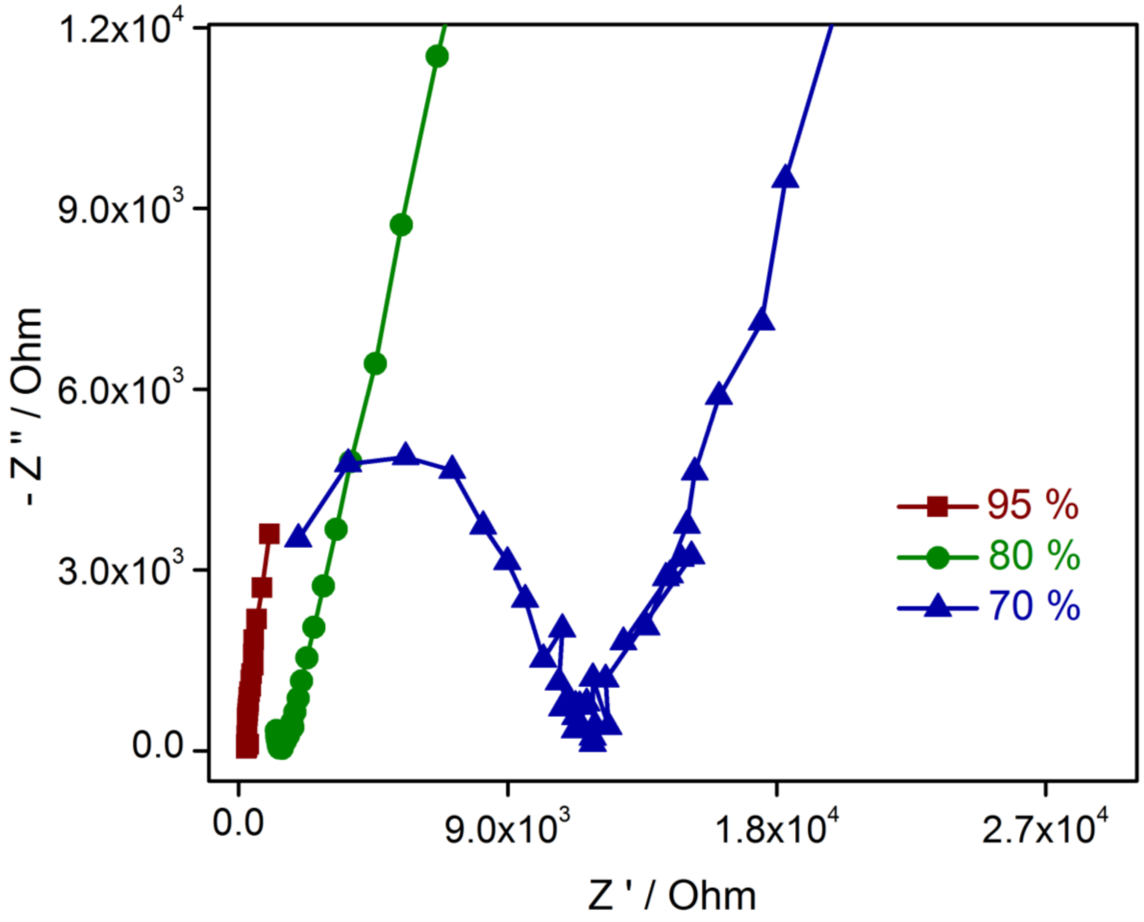

Figure S15: Humidity dependent impedance spectra of PCF-1 at 30 °C.

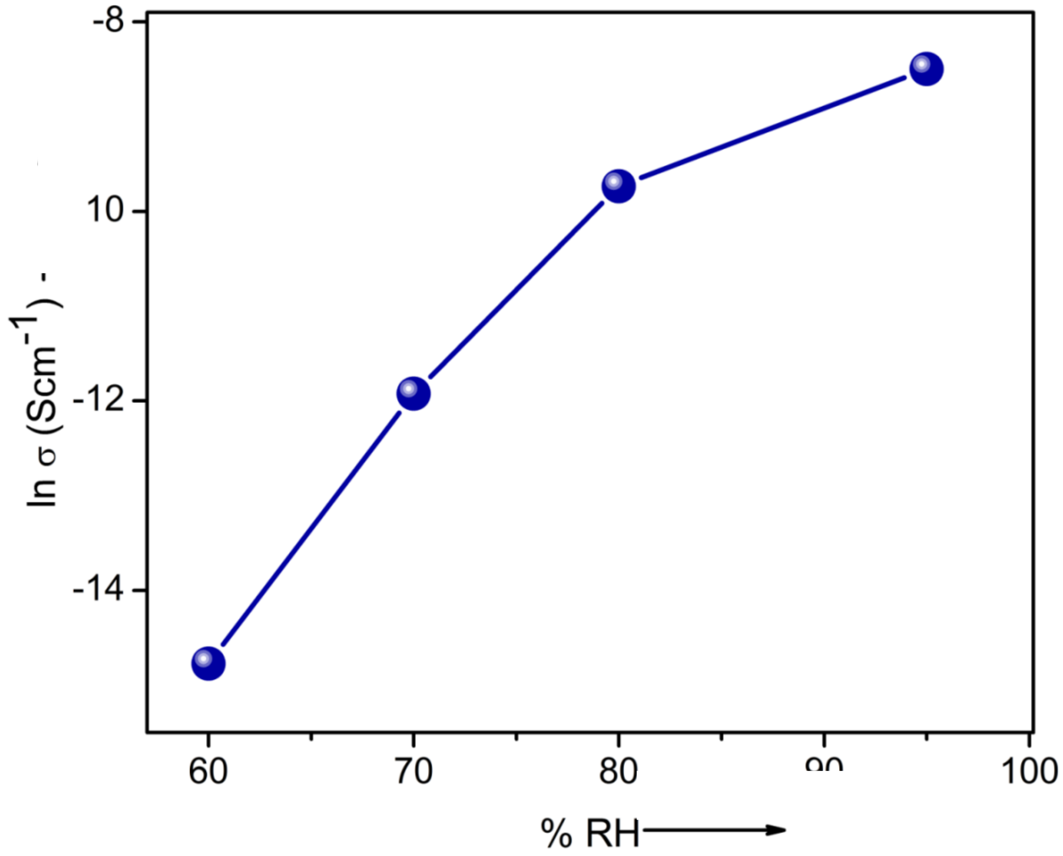

Figure S16: Humidity dependent proton conductivity of PCF-1 at 30 °C.

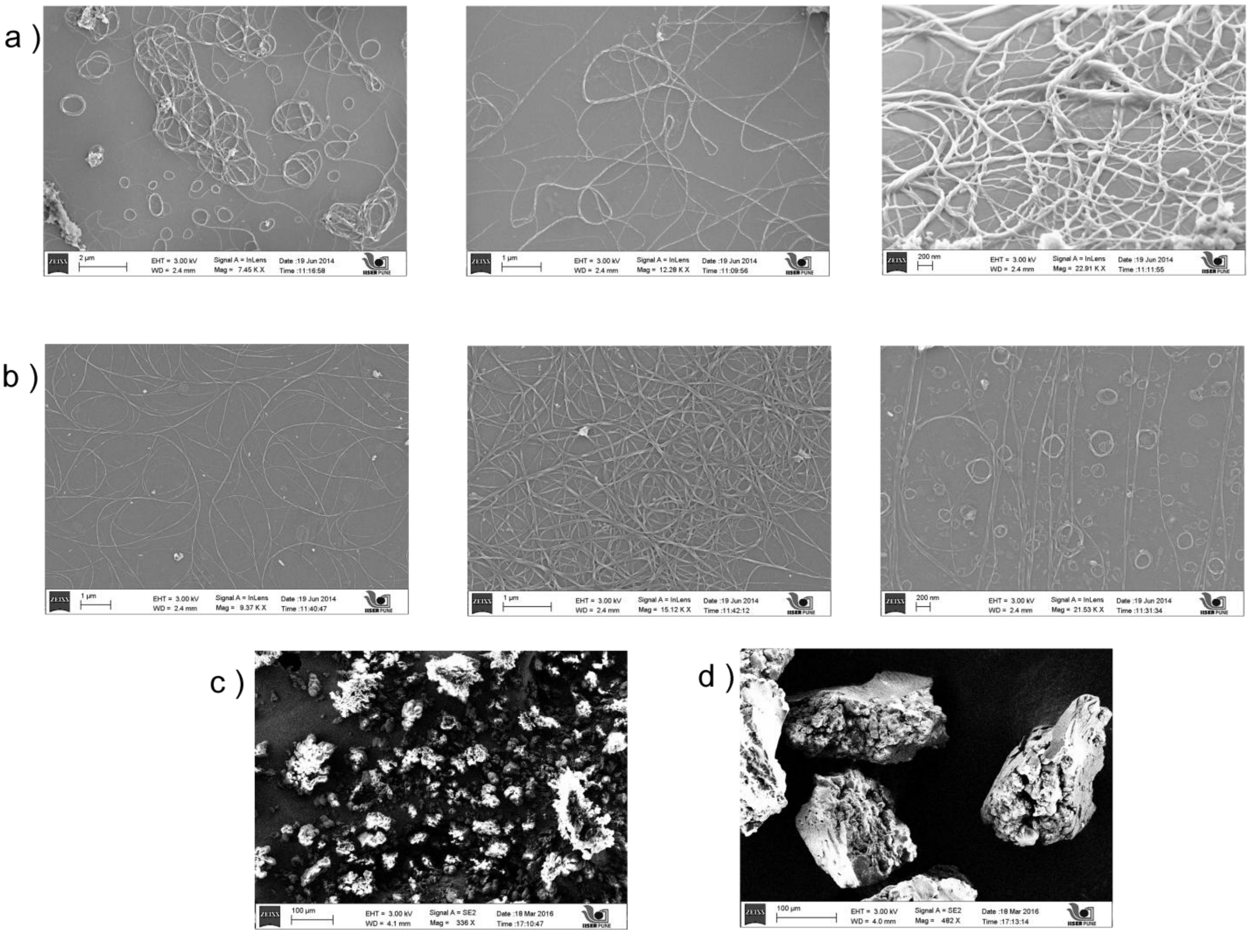

Figure S17: SEM images of a) PCF-1, b) PCF-1-SO_3H dispersed in $CHCl_3$; solid state SEM images of c) PCF-1 and d) PCF-1-SO_3H. Here, a) - b) are showing the fibril network of the both the compounds which is result of dispersion in the solvent ($CHCl_3$); c) - d) Agglomeration in the solid state leading to the formation of large solid particles of PCF-1 & PCF-1-SO_3H.

a)

Element	Weight%	Atomic%
C K	49.03	55.23
N K	13.61	13.15
O K	37.55	31.76
F K	-0.19	-0.13
Totals	100.00	

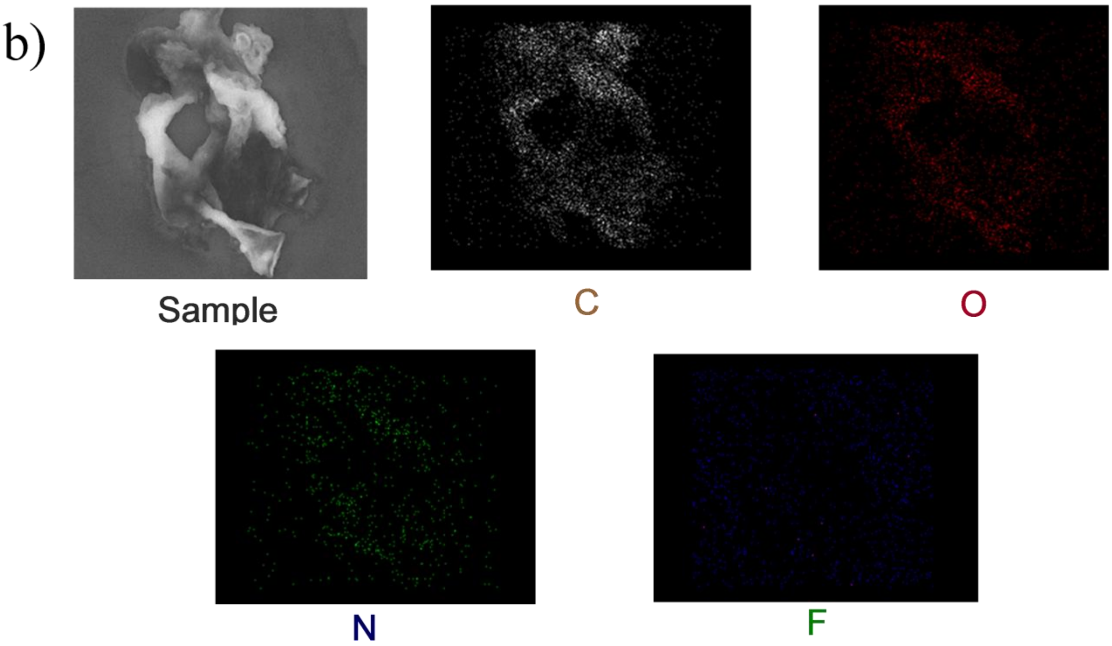

Figure S18: EDX analysis of PCF-1; a) % of corresponding elements and b) elemental mapping.

a)

Element	Weight%	Atomic%
C K	49.75	56.87
N K	4.37	4.16
O K	46.16	39.62
F K	-1.80	-1.30
S K	1.52	0.64
Totals	100.00	

b)

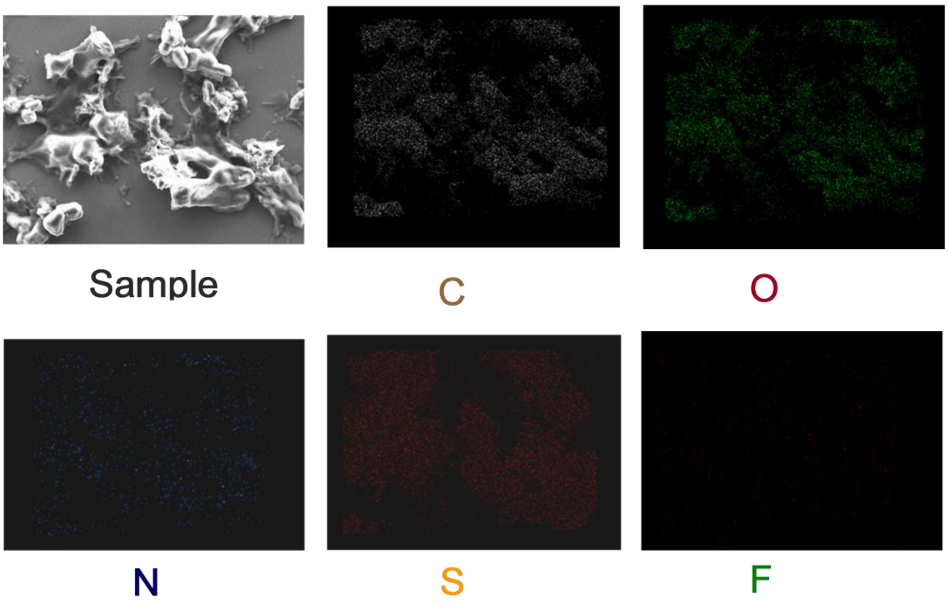

Figure S19: EDX analysis of PCF-1-SO_3H; a) % of corresponding elements and b) elemental mapping.

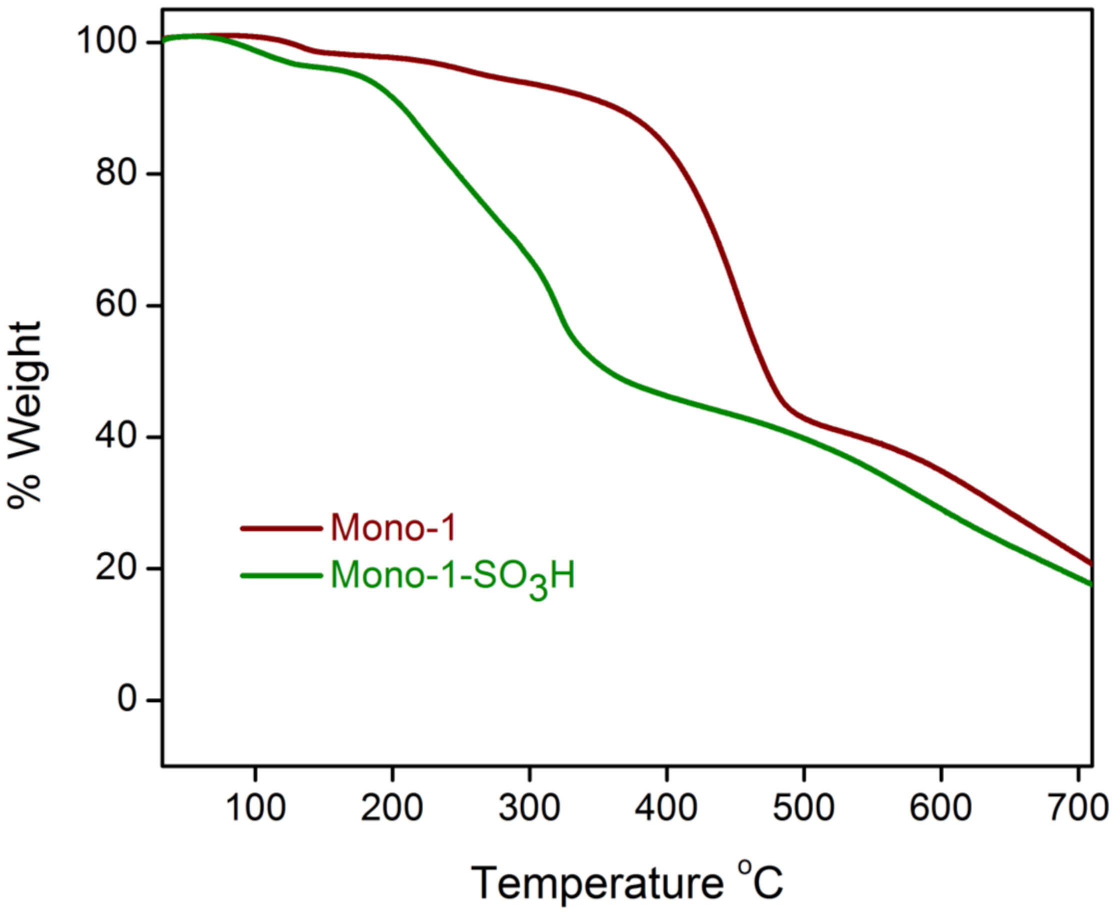

Figure S20: Thermo-gravimetric analysis (TGA) of Mono-1 and Mono-1-SO_3H.

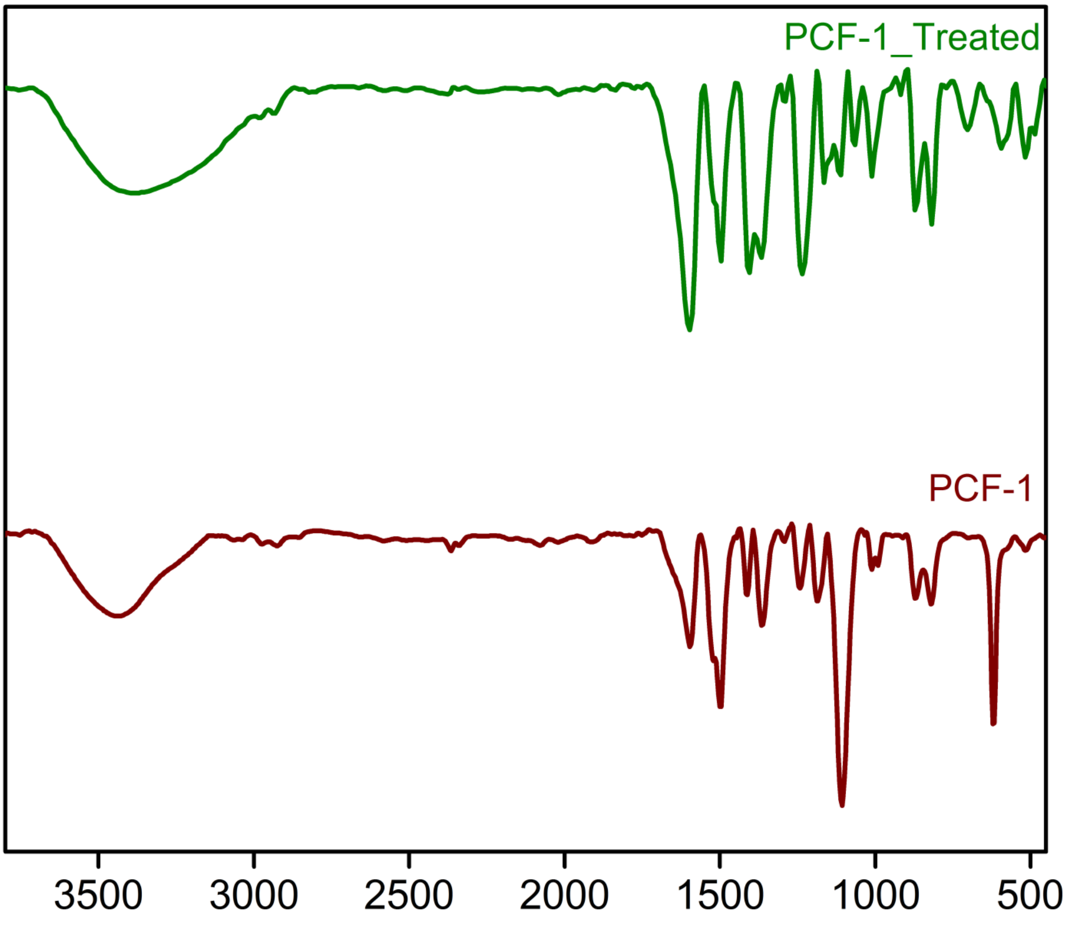

Figure S21: FT-IR spectra of PCF-1 (wine) and PCF-1 Fenton's reagent treated (green).

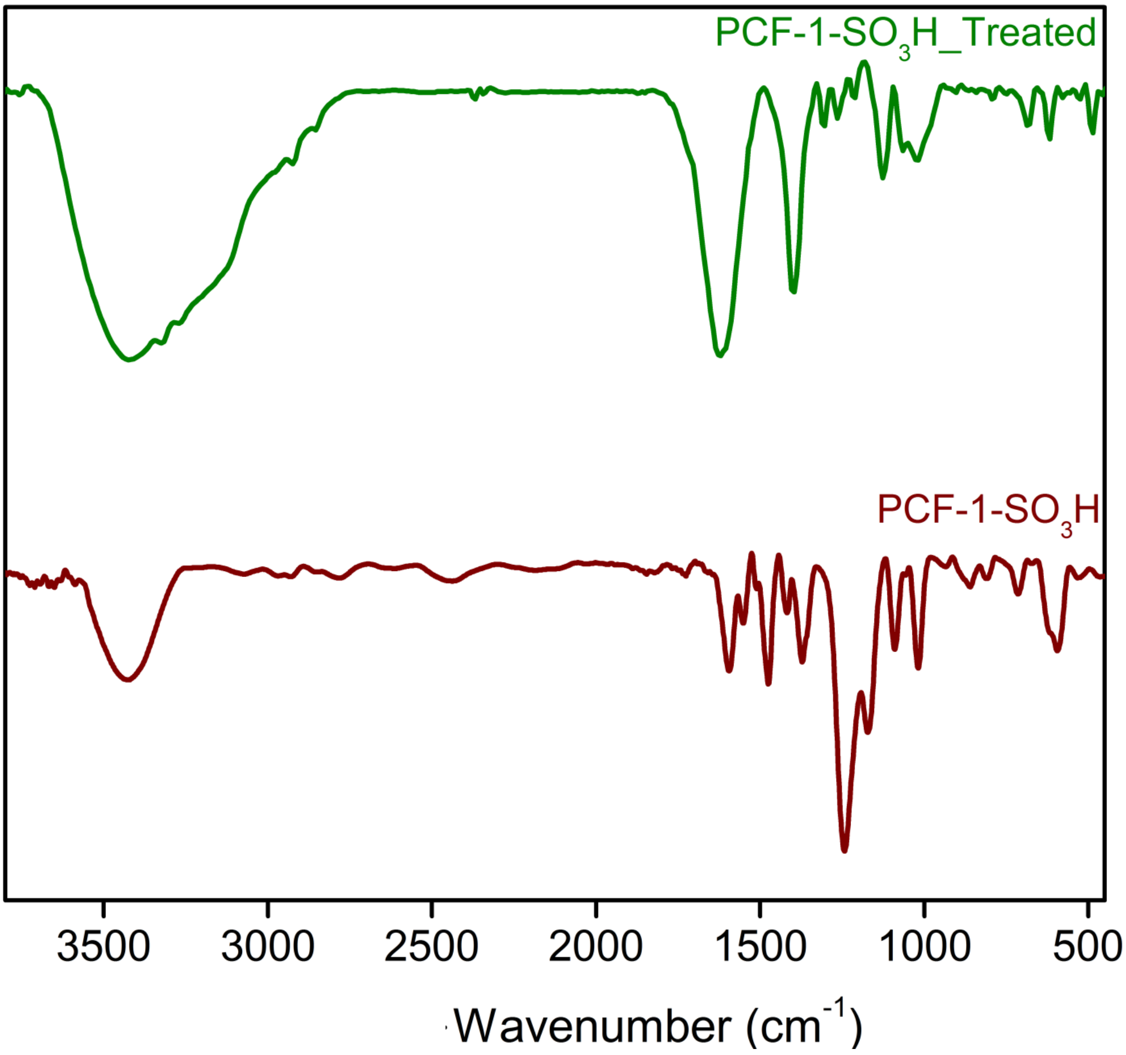

Figure S22: FT-IR spectra of PCF-1-SO$_3$H (wine) and PCF-1-SO$_3$H Fenton's reagent treated (green).

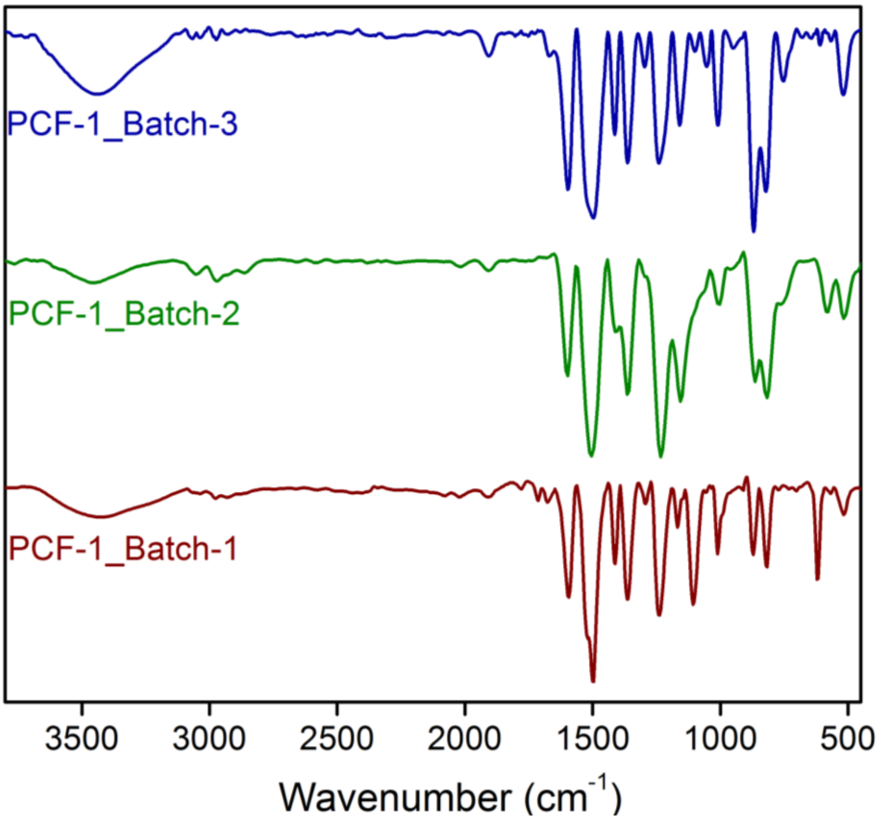

Figure S23: FT-IR spectra of 1st batch PCF-1 (wine red), 2nd batch PCF-1 (green) and 3rd batch of PCF-1 (blue).

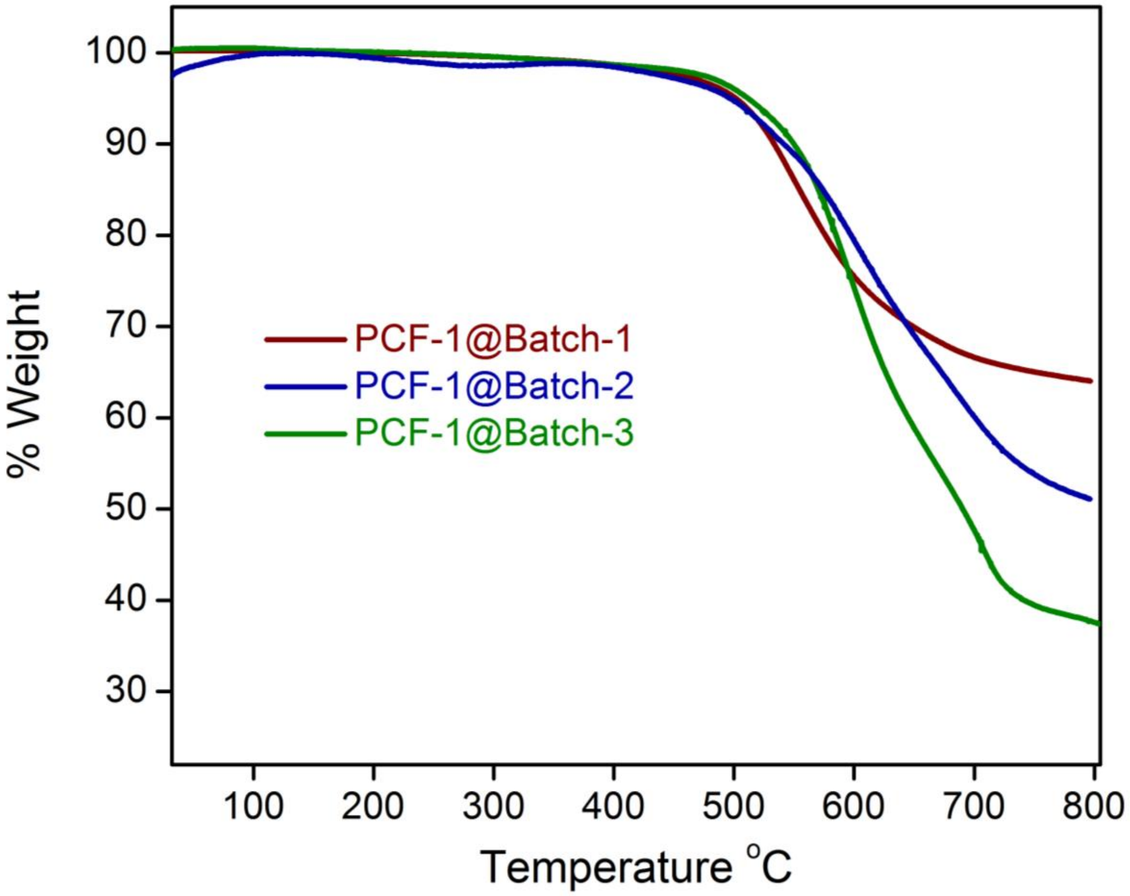

Figure S24: TGA profiles of 1st batch PCF-1 (wine red), 2nd batch PCF-1 (blue) and 3rd batch PCF-1 (green).

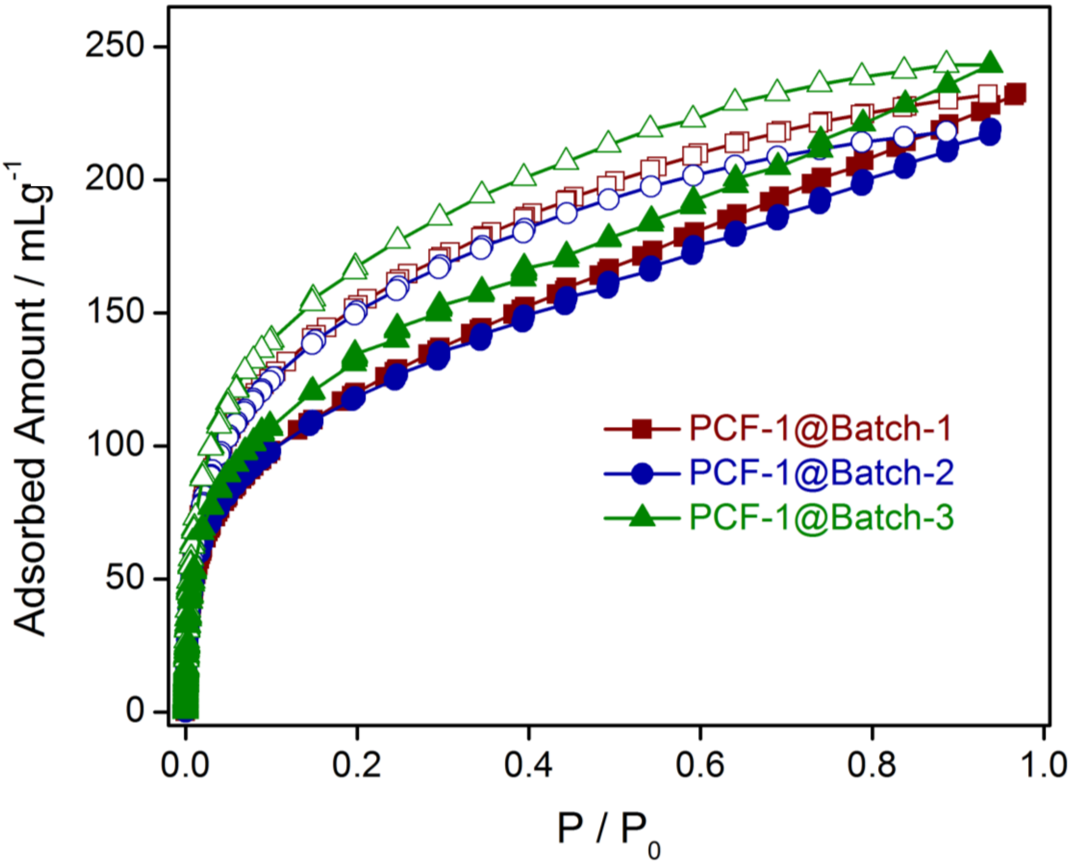

Figure S25: CO_2 adsorption of 1st batch PCF-1 (wine red), 2nd batch PCF-1 (blue) and 3rd batch PCF-1 (green) at 195 K.

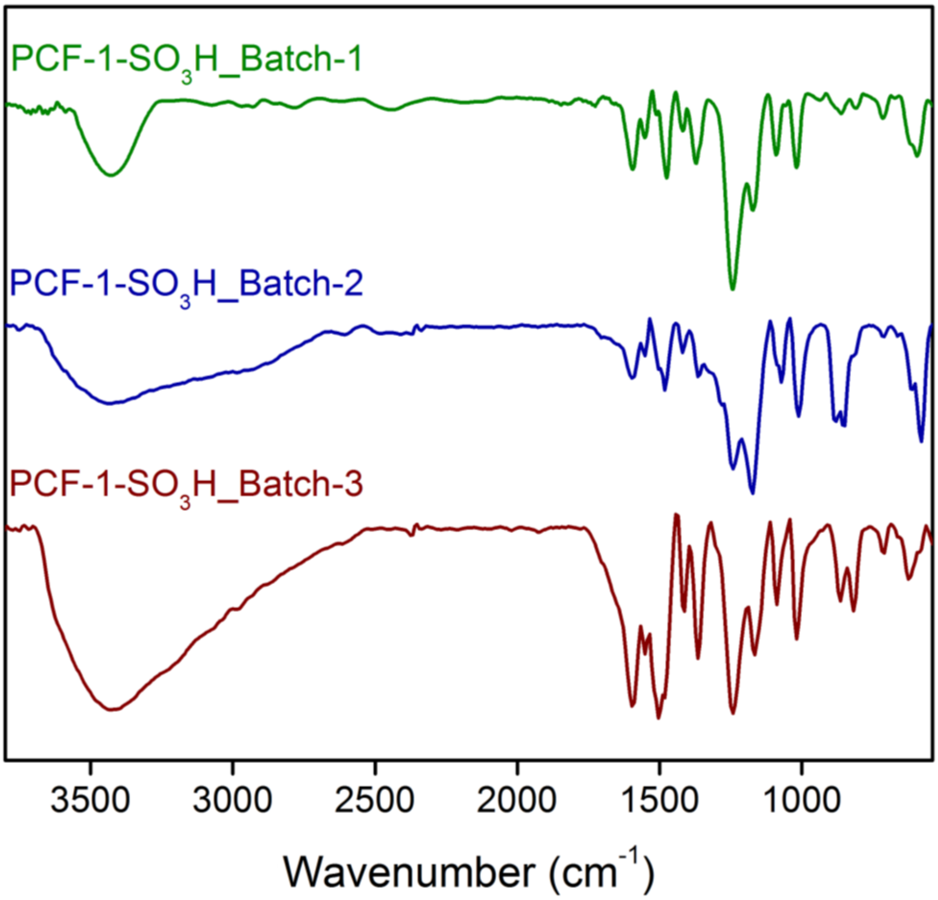

Figure S26: FT-IR spectra of 1st batch PCF-1-SO$_3$H (wine red), 2nd batch PCF-1-SO$_3$H (blue) and 3rd batch PCF-1-SO$_3$H (green).

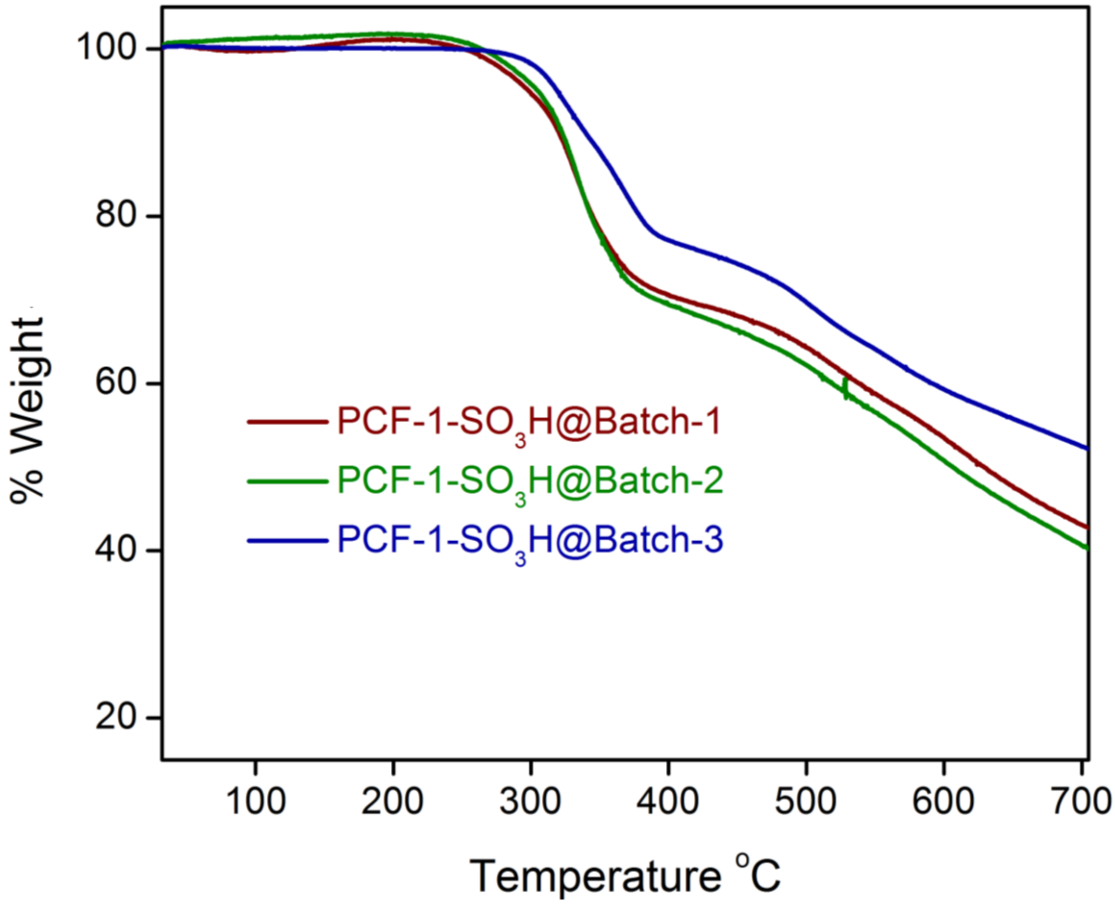

Figure S27: TGA profiles of 1st batch PCF-1-SO_3H (wine red), 2nd batch PCF-1-SO_3H (green) and 3rd batch PCF-1-SO_3H (blue).

Compound	% C	% H	% N	% S
PCF-1@Batch-1	77.84	2.594	7.57	0.0
PCF-1@Batch-2	77.58	3.112	7.45	0.0
PCF-1@Batch-3	74.59	4.245	6.76	0.0

Table S1: Elemental analysis data of three different batches of PCF-1.

Compound	% C	% H	% N	% S
PCF-1-SO_3H@Batch-1	54.20	3.512	5.59	6.482
PCF-1-SO_3H@Batch-2	53.82	3.276	4.96	7.573
PCF-1-SO_3H@Batch-3	55.46	3.421	5.00	6.769

Table S2: Elemental analysis data of three different batches of PCF-1-SO_3H.

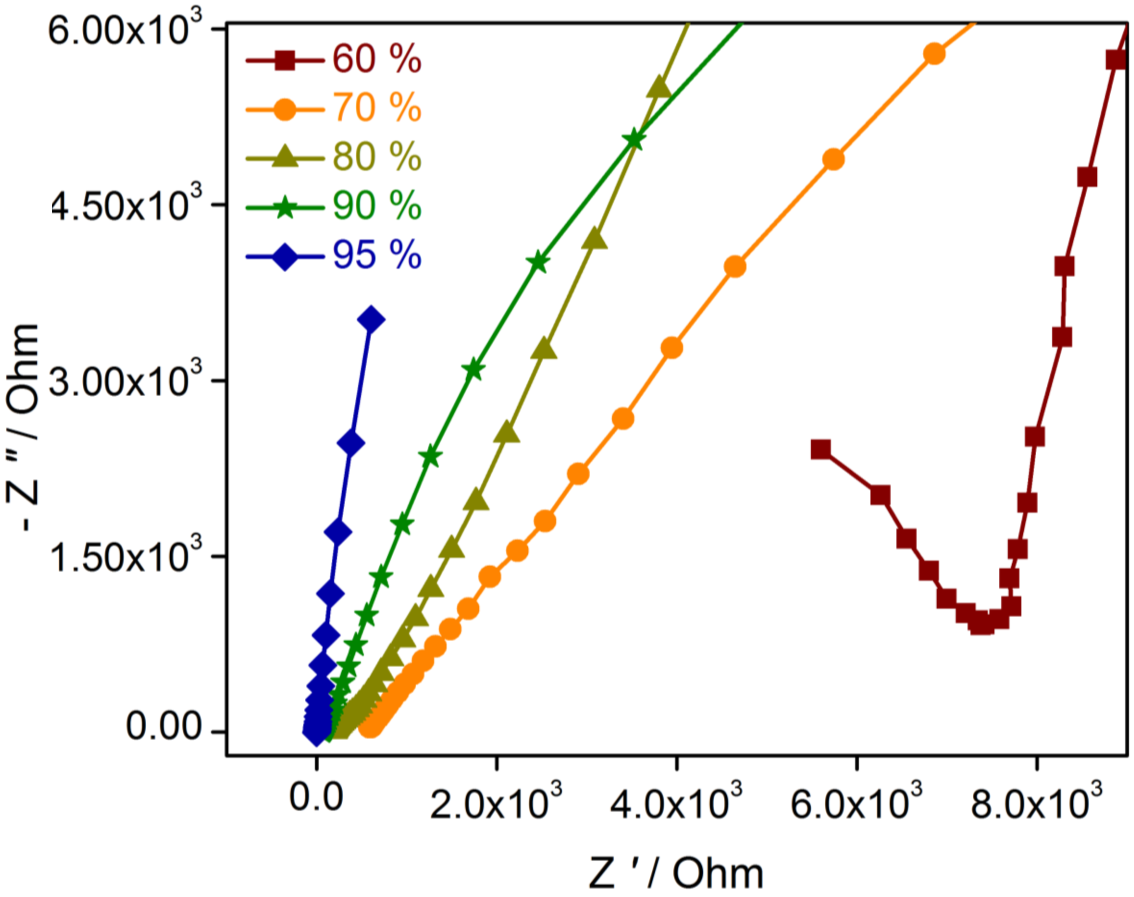

Figure S28: Humidity dependent impedance spectra of PCF-1-SO_3H at 30 °C.

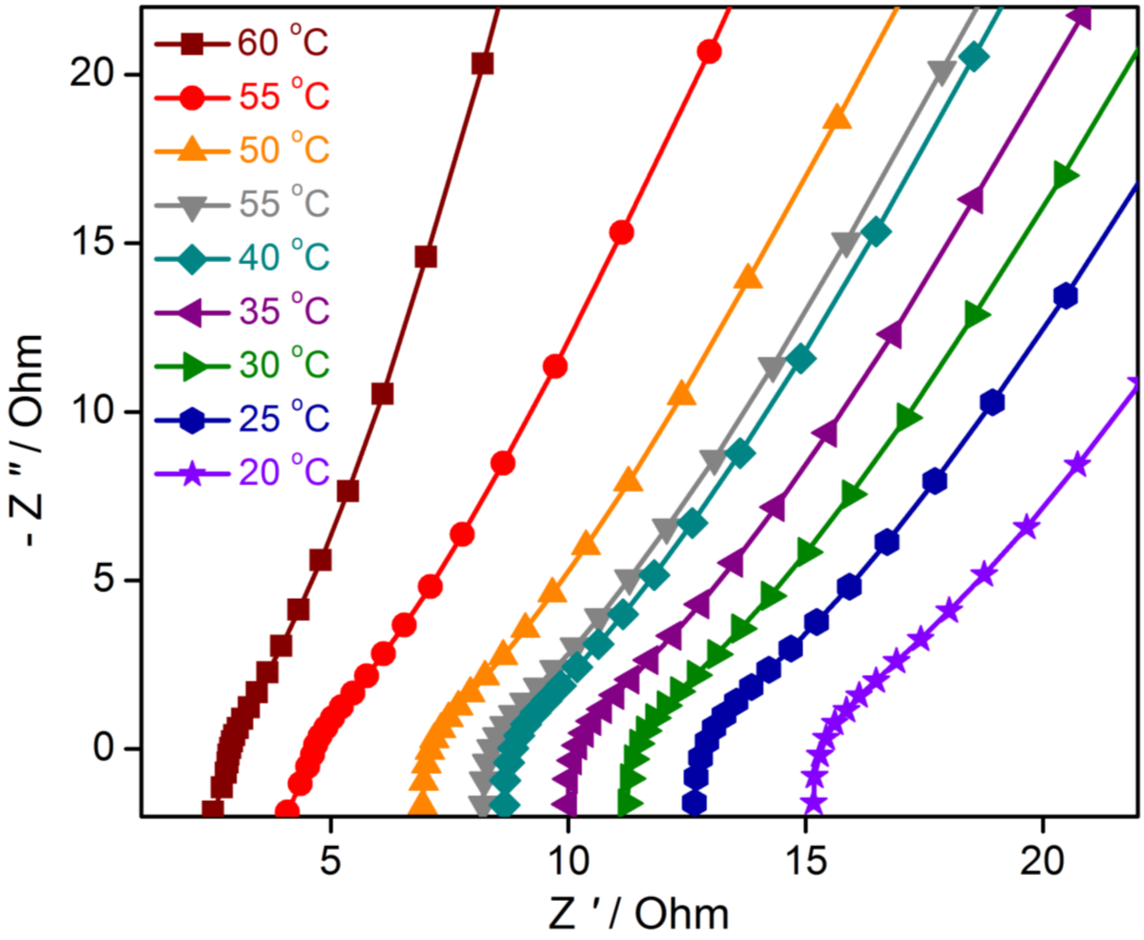

Figure S29: Temperature dependent impedance spectra of PCF-1-SO_3H at 95% RH.

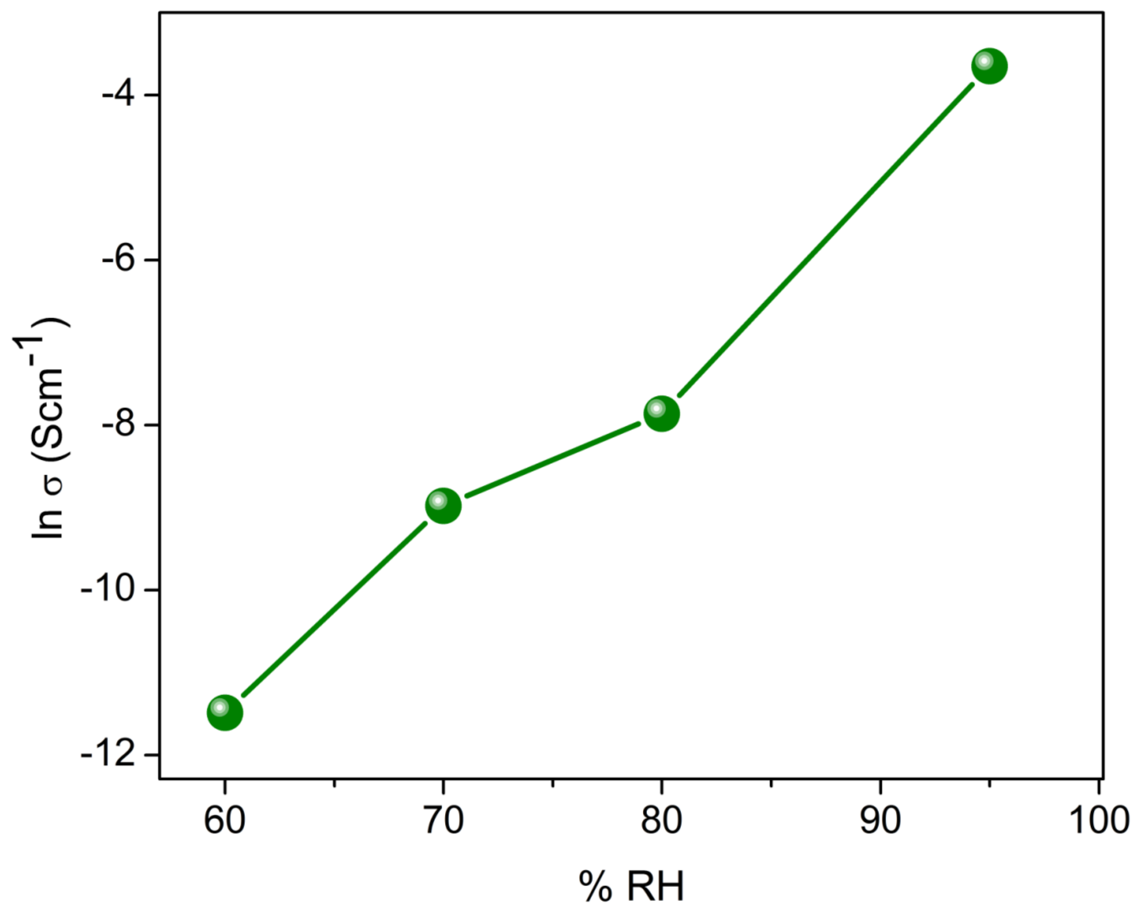

Figure S30: Humidity dependent proton conductivity of PCF-1-SO_3H at 30 °C.

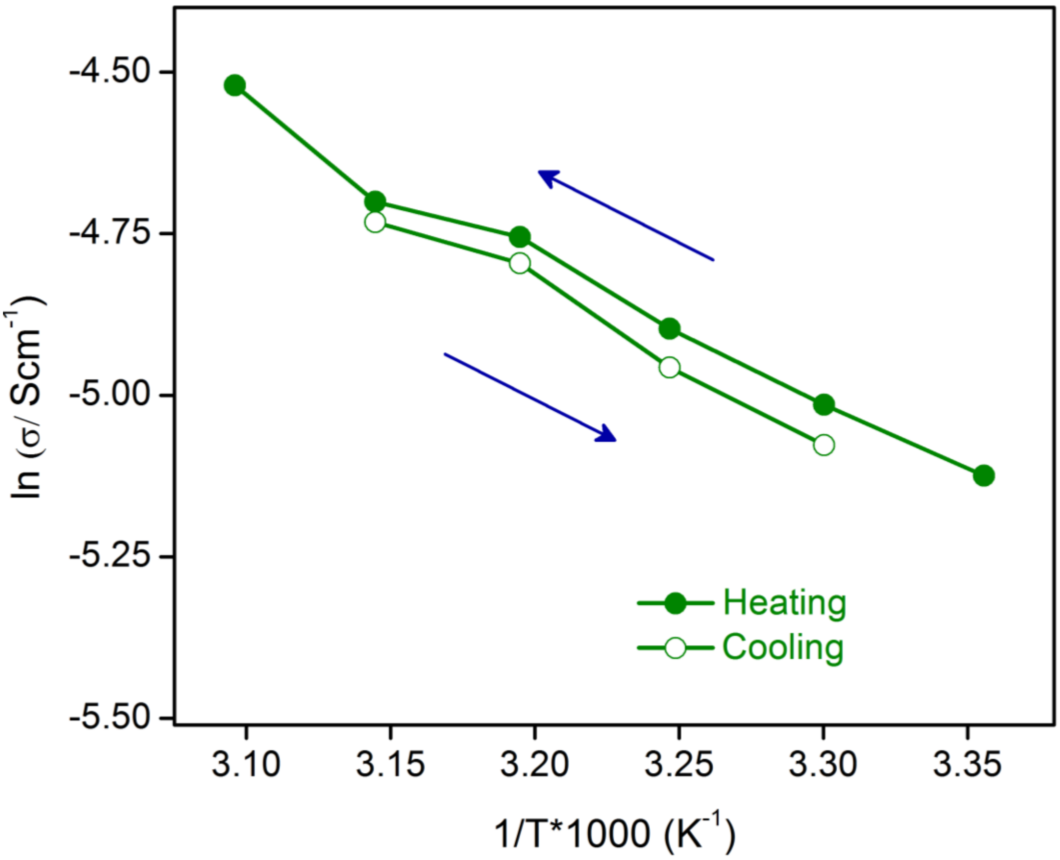

Figure S31: Arrhenius plot of PCF-1-SO_3H.

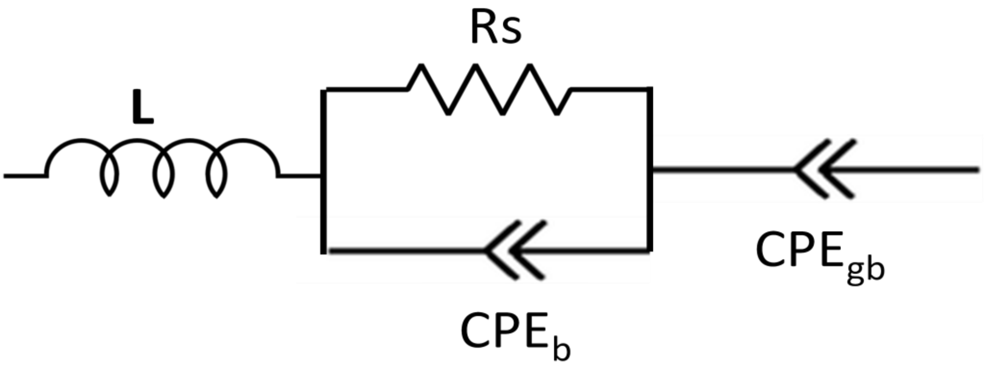

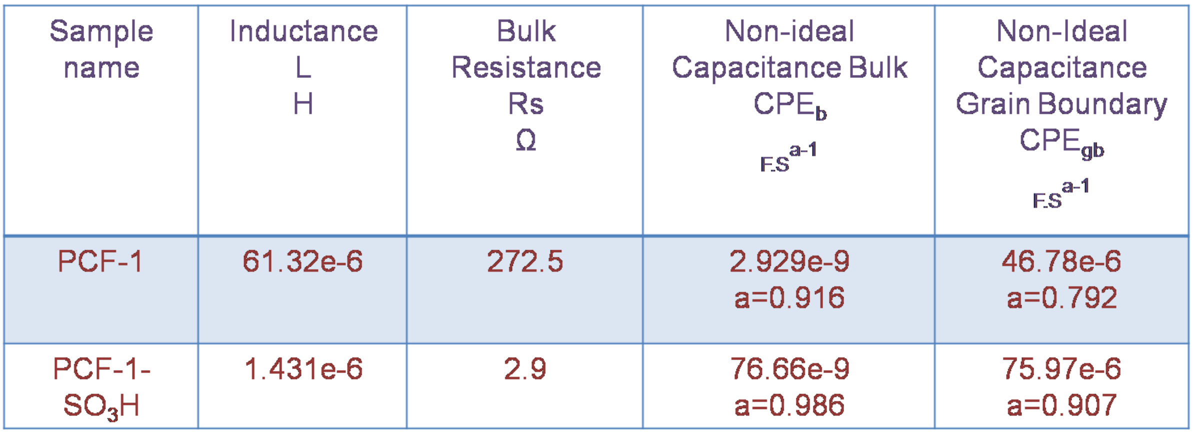

Sample name	Inductance L H	Bulk Resistance Rs Ω	Non-ideal Capacitance Bulk CPE_b $F.S^{a-1}$	Non-Ideal Capacitance Grain Boundary CPE_{gb} $F.S^{a-1}$
PCF-1	61.32e-6	272.5	2.929e-9 a=0.916	46.78e-6 a=0.792
PCF-1-SO_3H	1.431e-6	2.9	76.66e-9 a=0.986	75.97e-6 a=0.907

Figure S32: Impedence analysis details of both the compounds PCF-1 and PCF-1-SO_3H along with circuit model.

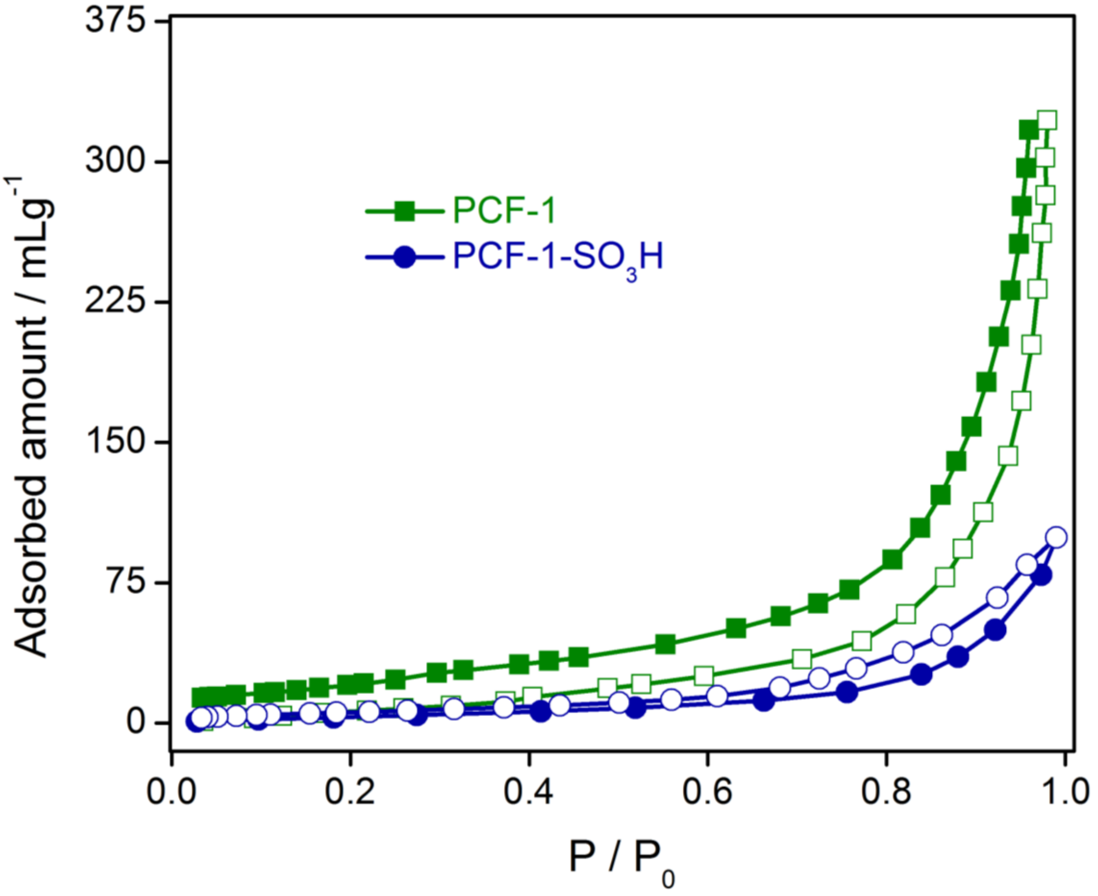

Figure S33: Water adsorption isotherm for PCF-1 (green) and PCF-1-SO_3H (blue) at 298 K.

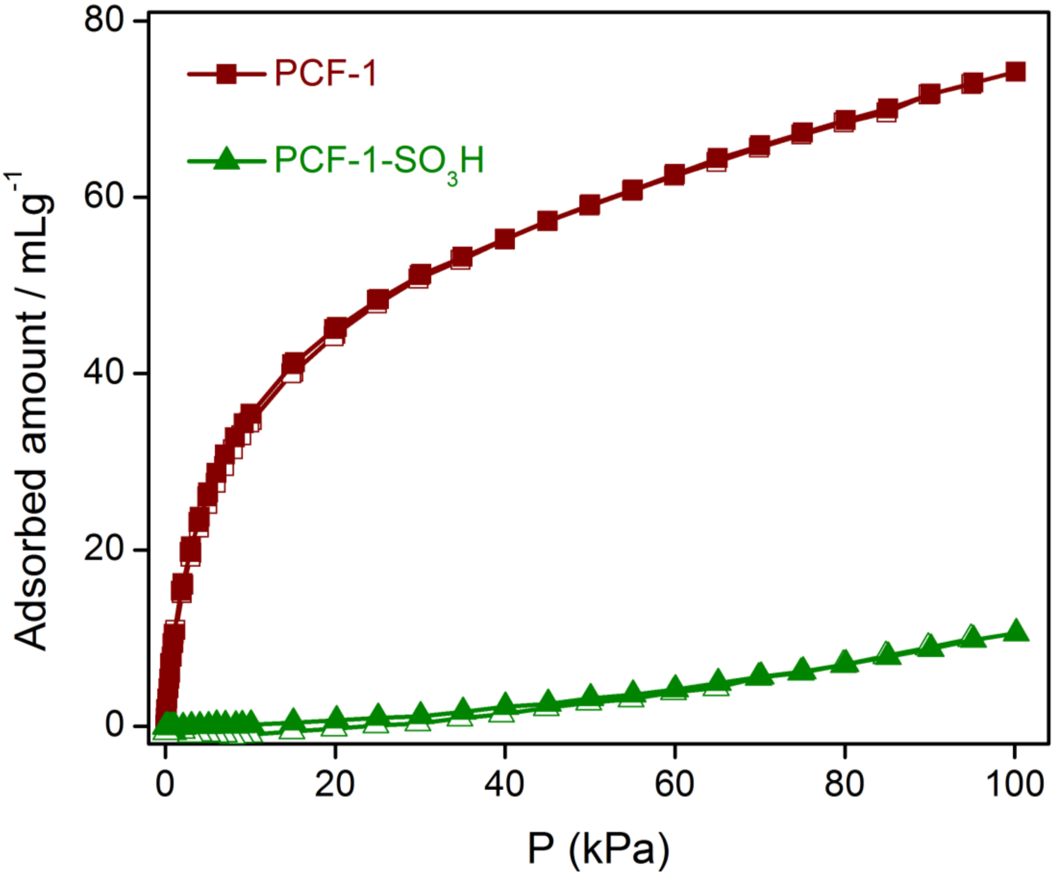

Figure S34: H_2 adsorption isotherm of PCF-1 (wine red) and PCF-1-SO_3H (green) at 77 K.

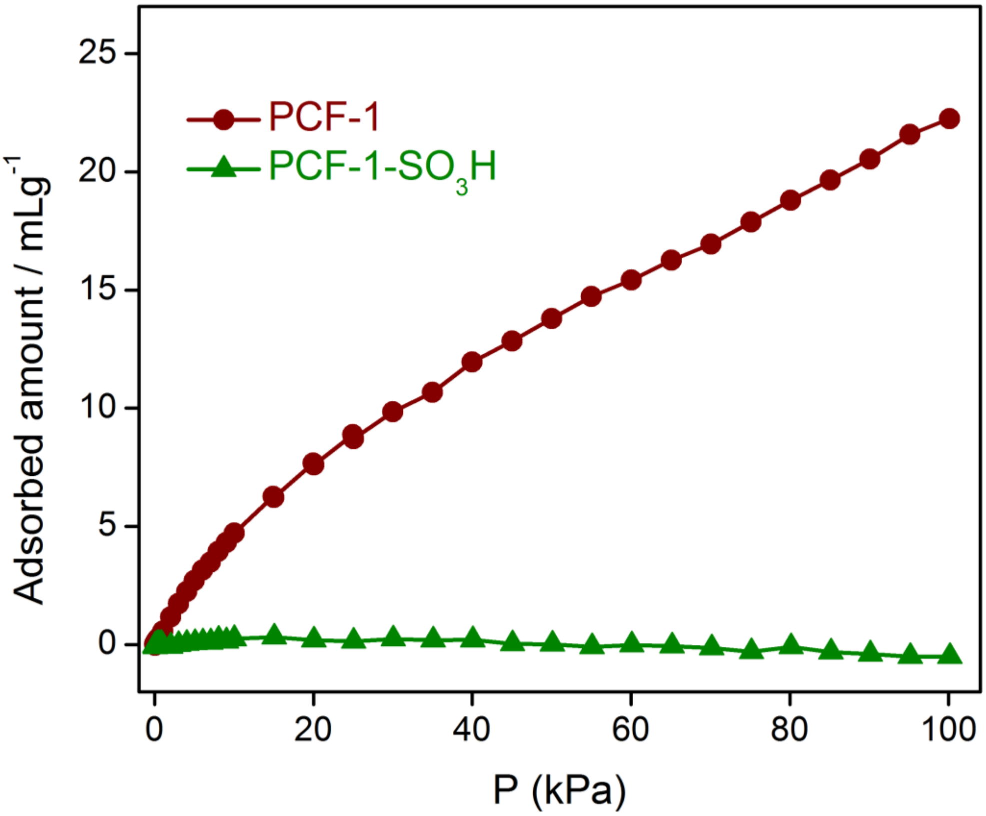

Figure S35: O_2 adsorption isotherm of PCF-1 (wine) and PCF-1-SO_3H (green) at 195 K.

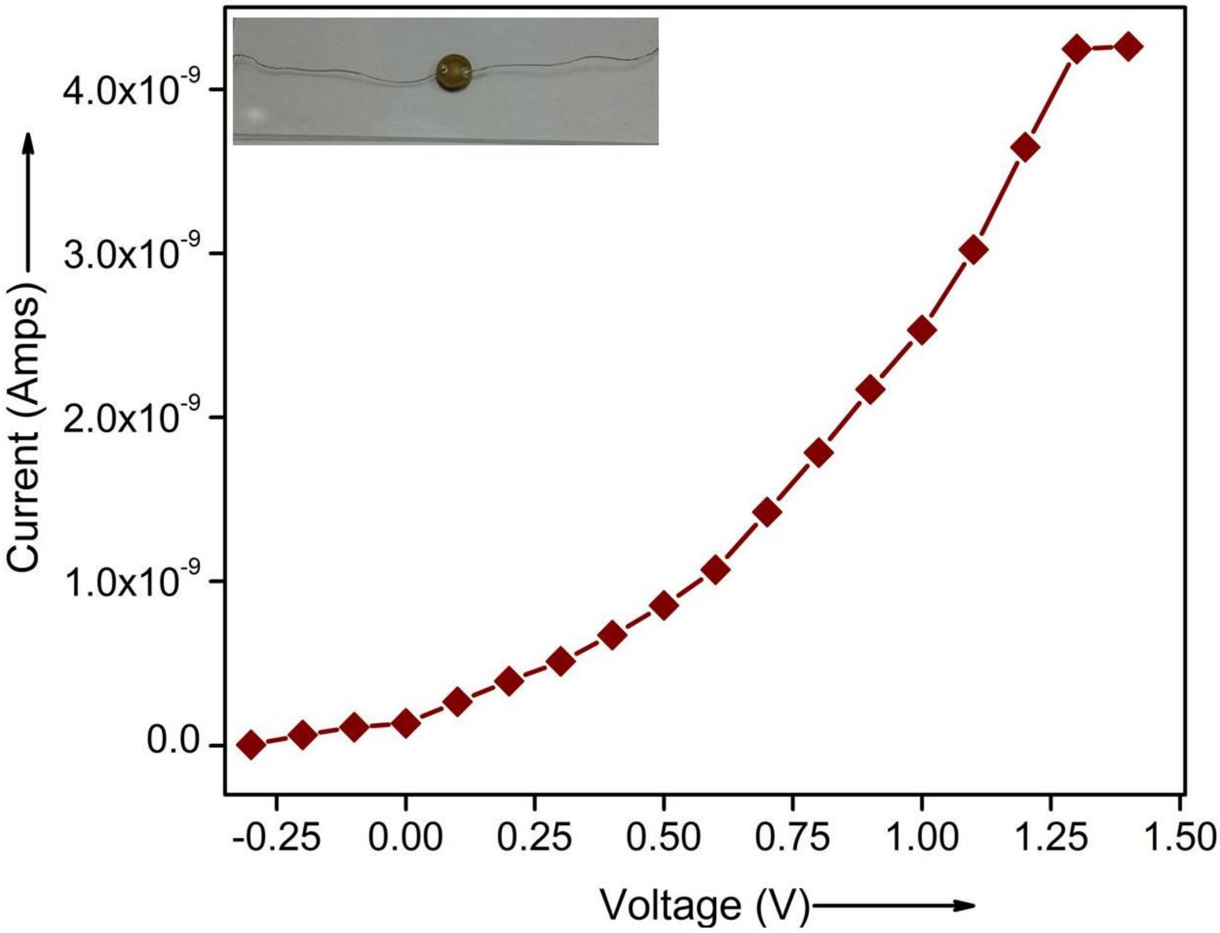

Figure S36: Electrical conductivity of PCF-1-SO_3H.

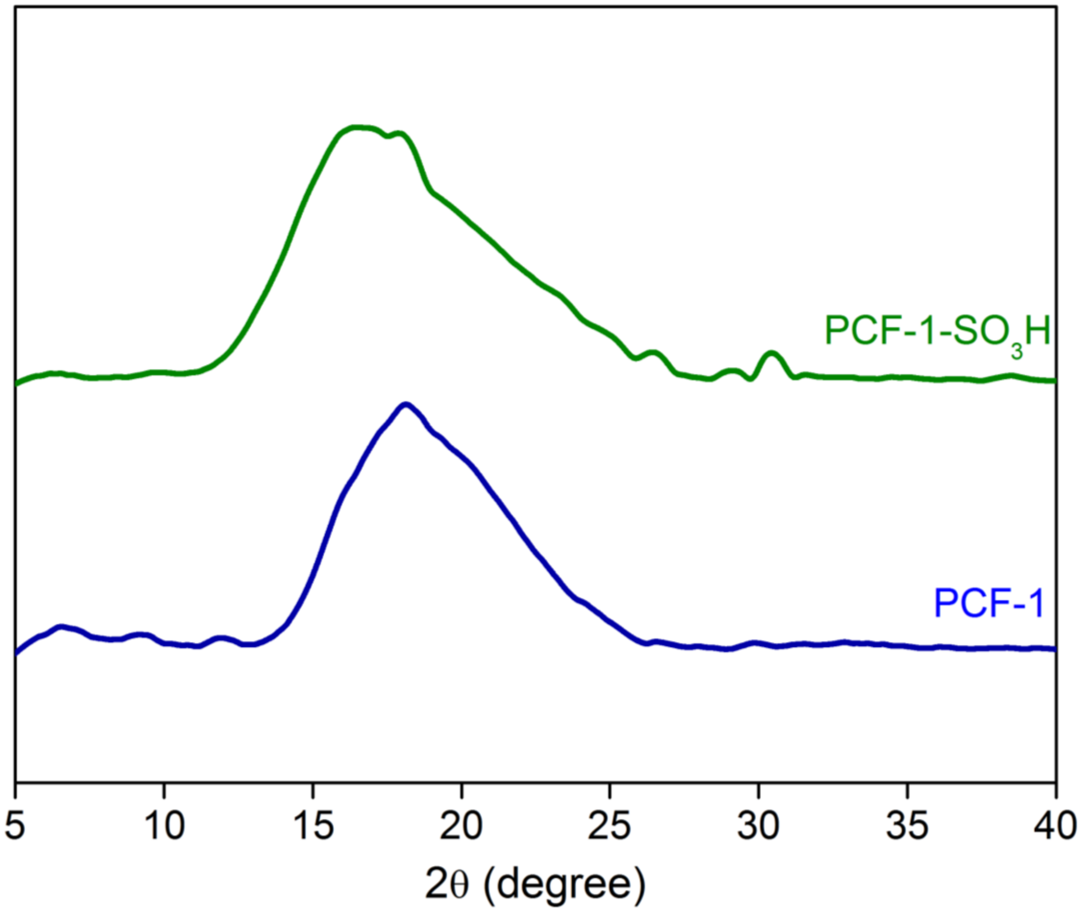

Figure S37: Powder X-ray diffraction of PCF-1 (blue) and PCF-1-SO$_3$H (green).

Table S3. Comparison of proton conductivity of PCF-1-SO$_3$H and PCF-1 with porous material based proton conductors:

Compounds	Conductivity (S cm^{-1})	Ea (eV)	Conditions	References
UiO-66(SO$_3$H)$_2$	8.4 x 10^{-2}	0.32	80 °C, 90% RH	1
TfOH@MIL-101	8 x 10^{-2}	0.18	60 °C, 15% RH	2
Fe-CAT-5	5 x 10^{-2}	0.24	25 °C, 98% RH	3
[(Me$_2$NH$_2$)$_3$(SO$_4$)]$_2$[Zn$_2$(ox)$_3$]	4.2 x 10^{-2}	0.13	25 °C, 98% RH	4
PCMOF-10	3.55 x 10^{-2}	0.4	70 °C, 95% RH	5
PCF-1-SO$_3$H	**2.6 x 10^{-2}**	**0.19**	**30 °C, 95% RH**	**This work**
H$^+$@Ni$_2$(dobdc)(H$_2$O)$_2$ (pH = 1.8)	2.2 x 10^{-2}	0.14	80 °C, 98% RH	6
PCMOF2^1/$_2$	2.1 x 10^{-2}	0.21	85 °C, 90% RH	7
[ImH$_2$][Cu(H$_2$PO4)$_{1.5}$(HPO$_4$)$_{0.5}$· Cl$_{0.5}$]	2 x 10^{-2}	1.1	130 °C, 0% RH	8
NUS-10(R)@PVDF-50	1.58 x 10^{-2}	0.21	80 °C, 97% RH	9
PA@TpBpy-MC	1.4 x 10^{-2}	0.11	59 °C, 98% RH	10
POF based 1S	1.3 x 10^{-2}	0.34	30 °C, 90% RH	11
H$_3$PO$_4$ @ MIL-101	1.0 x 10^{-2}	0.25	140 °C, 1.1% RH	12
H$_2$SO$_4$ @ MIL-101	1.0 x 10^{-2}	0.42	150 °C, 0.13% RH	12
CsHSO$_4$@Cr-MIL-101	10^{-2}	NA	200 °C, 0% RH	13
(NH$_4$)$_2$(H$_2$adp)[Zn$_2$(ox)$_3$]·3H$_2$O	8 x 10^{-3}	0.63	25 °C, 98% RH	14
Ca-PiPhtA-NH$_3$	6.6 x 10^{-3}	0.4	24 °C, 98% RH	15
im@TPB-DMTP-COF	4.37 x 10^{-3}	0.38	130 °C, 0% RH	16
PCMOF-5	4 x 10^{-3}	0.16	62 °C, 98% RH	17
Cu−TCPP nano-sheet	3.9 x 10^{-3}	0.28	25 °C, 98% RH	18
Sulfonated MIL-53(Al)	~3 x 10^{-3}	NA	~ 65 °C, <10% RH	19
[{(Zn$_{0.25}$)$_8$(O)}Zn$_6$(L)$_{12}$(H$_2$O)$_{29}$(DMF)$_{69}$(NO$_3$)$_2$]$_n$	2.3 x 10^{-3}	0.22	25 °C, 95% RH	20
Histamine@[Al(μ$_2$-OH)(1,4-NDC)]$_n$	1.7 x 10^{-3}	0.25	150 °C, 0% RH	21
HPF2–100	1.38 x 10^{-3}	0.10	90 °C, 90% RH	22
PA@Tp-Azo	9.9 × 10^{-4}	0.11	59 °C, 98% RH	23
phytic@TpPa-(SO$_3$H-Py)	5 × 10^{-4}	0.16	120 °C, 0% RH	24
1,2,4-Triazole @ β-PCMOF2	5 x 10^{-4}	0.34	150 °C, 0% RH	25
Im@Td-PPI	3.49×10^{-4}	0.30	90 °C, 0% RH	26
PCF-1	**2.03 x 10^{-4}**	**0.18**	**30 °C, 95% RH**	**This work**
Imidazole@[Al(μ2-OH)(1,4-ndc)]n	2.2 x 10^{-5}	0.6	120 °C, 0% RH	27

Table S2. Crystal data and structure refinement for Mono1.

Identification code	Mono1	
Empirical formula	$C_{42} H_{33} N_3 O_6$	
Formula weight	675.71	
Temperature	150(2) K	
Wavelength	0.71073 Å	
Crystal system	"Monoclinic"	
Space group	*C 2/c*	
Unit cell dimensions	a = 26.787(4) Å	α= 90°.
	b = 15.382(2) Å	ß= 118.439(3)°.
	c = 20.723(3) Å	ɣ = 90°.
Volume	7507.8(18) $Å^3$	
Z	8	
Density (calculated)	1.196 Mg/m^3	
Absorption coefficient	0.081 mm^{-1}	
F(000)	2832	
Theta range for data collection	1.581 to 28.484°.	
Index ranges	-35<=h<=35, -20<=k<=20, -27<=l<=22	
Reflections collected	65003	
Independent reflections	9409 [R(int) = 0.0578]	
Completeness to theta = 25.242°	99.8 %	
Refinement method	Full-matrix least-squares on F^2	
Data / restraints / parameters	9409 / 6 / 451	
Goodness-of-fit on F^2	0.958	
Final R indices [I>2sigma(I)]	R1 = 0.1250, wR2 = 0.3296	
R indices (all data)	R1 = 0.1509, wR2 = 0.3445	
Extinction coefficient	n/a	
Largest diff. peak and hole	0.847 and -0.831 e.$Å^{-3}$	

References:

1. W. J. Phang, H. Jo, W. R. Lee, J. H. Song, K. Yoo, B. Kim and C. S. Hong, *Angew. Chem. Int. Ed.*, 2015, **54**, 5142.

2. D. N. Dybtsev, V. G. Ponomareva, S. B. Aliev, A. P. Chupakhin, M. R. Gallyamov, N. K. Moroz, B. A. Kolesov, K. A. Kovalenko, E. S. Shutova and V. P. Fedin, *ACS Appl. Mater. Interfaces*, 2014, **6**, 5161.

3. N. T. T. Nguyen, H. Furukawa, F. Gándara, C. A. Trickett, H. M. Jeong, K. E. Cordova and O. M. Yaghi, *J. Am. Chem. Soc.*, 2015, **137**, 15394.

4. S. S. Nagarkar, S. M. Unni, A. Sharma, S. Kurungot and S. K. Ghosh, *Angew. Chem. Int. Ed.*, 2014, **53**, 2638.

5. P. Ramaswamy, N. E. Wong, B. S. Gelfand and G. K. H. Shimizu, *J. Am. Chem. Soc.*, 2015, **137**, 7640.

6. W. J. Phang, W. R. Lee, K. Yoo, D. W. Ryu, B. Kim and C. S. Hong, *Angew. Chem. Int. Ed.*, 2014, **53**, 8383.

7. S. Kim, K. W. Dawson, B. S. Gelfand, J. M. Taylor and G. K. H. Shimizu, *J. Am. Chem. Soc.*, 2013, **135**, 963.

8. S. Horike, W. Chen, T. Itakura, M. Inukai, D. Umeyama, H. Asakurae and S. Kitagawa, *Chem. Commun.*, 2014, **50**, 10241.

9. Y. Peng, G. Xu, Z. Hu, Y. Cheng, C. Chi, D. Yuan, H. Cheng and D. Zhao, *ACS Appl. Mater. Interfaces* 2016, **8**, 18505.

10. D. B. Shinde, H. B. Aiyappa, M. Bhadra, B. P. Biswal, P. Wadge, S. Kandambeth, B. Garai, T. Kundu, S. Kurungot and R. Banerjee, *J. Mater. Chem. A*, 2016, **4**, 2682.

11. D. W. Kang, K. S. Lim, K. J. Lee, J. H. Lee, W. R. Lee, J. H. Song, K. H. Yeom, J. Y. Kim and C. S. Hong, *Angew. Chem. Int. Ed.*, 2016, **55**, 16123.

12. V. G. Ponomareva, K. A. Kovalenko, A. P. Chupakhin, D. N. Dybtsev, E. S. Shutova and V. P. Fedin, *J. Am. Chem. Soc.*, 2012, **134**, 15640.

13. V. G. Ponomareva, K. A. Kovalenko, A. P. Chupakhin, E. S. Shutova and V. P. Fedin, *Solid State Ionics*, 2012, **225**, 420.

14. M. Sadakiyo, T. Yamada, H. Kitagawa and *J. Am. Chem. Soc.*, 2009, **131**, 9906.

15. M. Bazaga-Garcia, R. M. Colodrero, M. Papadaki, P. Garczarek, J. Zon, P. Olivera-Pastor, E. R. Losilla, L. Leon-Reina, M. A. Aranda, D. Choquesillo-Lazarte, K. D. Demadis and A. Cabeza, *J. Am. Chem. Soc.*, 2014*,* **136***,* 5731.

16. H. Xu, S. Tao and D. Jiang, *Nat. Mater.*, 2016, (DOI: 10.1038/NMAT4611).

17. J. M. Taylor, K. W. Dawson and G. K. H. Shimizu, *J. Am. Chem. Soc.*, 2013, **135**, 1193.

18. G. Xu, K. Otsubo, T. Yamada, S. Sakaida and H. Kitagawa, *J. Am. Chem. Soc.*, 2013, **135**, 7438.

19. M. G. Goesten, J. Juan-Alcañiz, E. V. Ramos-Fernandez, K. B. S. S. Gupta, E. Stavitski, H. van Bekkum, J. Gascon and F. Kapteijn, *J. Catal.*, 2011, **281**, 177.

20. S. Sen, N. N. Nair, T. Yamada, H. Kitagawa and P. K. Bharadwaj, *J. Am. Chem. Soc.I,* 2012, **134**, 19432.

21. D. Umeyama, S. Horike, M. Inukai, Y. Hijikata and S. Kitagawa, *Angew. Chem., Int. Ed.*, 2011, **50**, 11706.

22. S. Nandi, V. M. Dhavale, S. Shalini, U. Werner-Zwanziger, H. Singh, S. Kurungot and R. Vaidhyanathan, *Adv. Mater. Interfaces*, 2015**,** (DOI: 10.1002/admi.201500301).

23. S. Chandra, T. Kundu, S. Kandambeth, R. BabaRao, Y. Marathe, S. M. Kunjir and R. Banerjee, *J. Am. Chem. Soc.*, 2014, **136**, 6570.

24. S. Chandra, T. Kundu, K. Dey, M. Addicoat, T. Heine and R. Banerjee, *Chem. Mater.*, 2016, **28**, 1489.

25. J. A. Hurd, R. Vaidhyanathan, V. Thangadurai, C. I. Ratcliffe, I. L. Moudrakovski and G. K. H. Shimizu, *Nat. Chem.*, 2009, **1**, 705.

26. Y. Ye, L. Zhang, Q. Peng, G. -E. Wang, Y. Shen, Z. Li, L. Wang, X. Ma, Q. -H. Chen, Z. Zhang and S. Xiang, *J. Am. Chem. Soc.*, 2015, **137**, 913.

27. S. Bureekaew, S. Horike, M. Higuchi, M. Mizuno, T. Kawamura, D. Tanaka, N. Yanai and S. Kitagawa, *Nat. Mater.*, 2009, **8**, 831.